JEM Journal of Experimental Medicine

ARTICLE

Germline-activating mutations in *PIK3CD* compromise B cell development and function

Danielle T. Avery[1*], Alisa Kane[1,2,3,4,5*], Tina Nguyen[1,2], Anthony Lau[1,2], Akira Nguyen[1,2], Helen Lenthall[1], Kathryn Payne[1], Wei Shi[6,7], Henry Brigden[1], Elise French[1], Julia Bier[1,2], Jana R. Hermes[1], David Zahra[1], William A. Sewell[1,2,8], Danyal Butt[1,2], Michael Elliott[9,10], Kaan Boztug[11,12,13], Isabelle Meyts[14], Sharon Choo[15], Peter Hsu[5,16], Melanie Wong[5,16], Lucinda J. Berglund[5,17,18], Paul Gray[5,19], Michael O'Sullivan[20], Theresa Cole[15], Steven M. Holland[21], Cindy S. Ma[1,2,5], Christoph Burkhart[22], Lynn M. Corcoran[6,7], Tri Giang Phan[1,2,5], Robert Brink[1,2,5], Gulbu Uzel[21], Elissa K. Deenick[1,2,5**], and Stuart G. Tangye[1,2,5**]

Gain-of-function (GOF) mutations in *PIK3CD*, encoding the p110δ subunit of phosphatidylinositide 3-kinase (PI3K), cause a primary immunodeficiency. Affected individuals display impaired humoral immune responses following infection or immunization. To establish mechanisms underlying these immune defects, we studied a large cohort of patients with *PIK3CD* GOF mutations and established a novel mouse model using CRISPR/Cas9-mediated gene editing to introduce a common pathogenic mutation in *Pik3cd*. In both species, hyperactive PI3K severely affected B cell development and differentiation in the bone marrow and the periphery. Furthermore, PI3K GOF B cells exhibited intrinsic defects in class-switch recombination (CSR) due to impaired induction of activation-induced cytidine deaminase (AID) and failure to acquire a plasmablast gene signature and phenotype. Importantly, defects in CSR, AID expression, and Ig secretion were restored by leniolisib, a specific p110δ inhibitor. Our findings reveal key roles for balanced PI3K signaling in B cell development and long-lived humoral immunity and memory and establish the validity of treating affected individuals with p110δ inhibitors.

Introduction

B cell development occurs in the bone marrow (BM) and involves the progressive maturation of pluripotent hematopoietic stem cells into populations of progenitor (pro-B), precursor (preB), and immature B cells (Uckun, 1990; LeBien and Tedder, 2008). The early stages of B cell development also require the rearrangement of genes encoding the B cell antigen (Ag) receptor (BCR), which is responsible for recognizing specific Ag (Uckun, 1990; LeBien and Tedder, 2008). Immature B cells that express a functional, nonself reactive BCR are then exported to the periphery as transitional B cells, where they undergo final maturation into immunocompetent naive B cells capable of surveying the host for the presence of foreign Ags (Goodnow, 2007).

While B cells play numerous roles in host defense against infection (LeBien and Tedder, 2008), their main function is to produce antibodies (Abs) that neutralize and clear invading pathogens from the host (Goodnow et al., 2010; Tangye et al., 2013, 2015). Following Ag stimulation, naive B cells rapidly become short-lived plasmablasts that localize to extrafollicular regions of lymphoid tissues, or they seed germinal centers (GCs) in lymphoid follicles where, with help from $CD4^+$ T cells, they undergo somatic hypermutation (SHM), affinity maturation,

[1]Immunology Division, Garvan Institute of Medical Research, Darlinghurst, New South Wales, Australia; [2]St. Vincent's Clinical School, University of New South Wales (UNSW), New South Wales, Australia; [3]Department of Immunology and Allergy, Liverpool Hospital, Liverpool, New South Wales, Australia; [4]South Western Sydney Clinical School, UNSW Sydney, Liverpool, New South Wales, Australia; [5]Clinical Immunogenomics Research Consortia Australia (CIRCA), Sydney, New South Wales, Australia; [6]Molecular Immunology and Bioinformatics Divisions, Walter & Eliza Hall Institute for Medical Research, Parkville, Victoria, Australia; [7]University of Melbourne, Parkville, Victoria, Australia; [8]Immunology Department, SydPath, St. Vincent's Hospital, Sydney, New South Wales, Australia; [9]Sydney Medical School, University of Sydney, Sydney, Australia; [10]Chris O'Brien Lifehouse Cancer Centre, Royal Prince Alfred Hospital, Sydney, Australia; [11]Ludwig Boltzmann Institute for Rare and Undiagnosed Diseases, Vienna, Austria; [12]CeMM Research Center for Molecular Medicine of the Austrian Academy of Sciences, Vienna, Austria; [13]St. Anna Children's Hospital and Children's Cancer Research Institute, Department of Pediatrics and Adolescent Medicine, Medical University of Vienna, Vienna, Austria; [14]Department of Immunology and Microbiology, Childhood Immunology, Department of Pediatrics, University Hospitals Leuven and KU Leuven, Leuven, Belgium; [15]Department of Allergy and Immunology, Royal Children's Hospital Melbourne, Victoria, Australia; [16]Children's Hospital at Westmead, New South Wales, Australia; [17]Immunopathology Department, Westmead Hospital, Westmead, New South Wales, Australia; [18]Faculty of Medicine, University of Sydney, Sydney, New South Wales, Australia; [19]University of New South Wales School of Women's and Children's Health, New South Wales, Australia; [20]Department of Immunology and Allergy, Princess Margaret Hospital, Subiaco, Western Australia, Australia; [21]Laboratory of Clinical Immunology and Microbiology, National Institutes of Allergy and Infectious Diseases, National Institutes of Health, Bethesda, MD; [22]Novartis Institutes for BioMedical Research, Novartis Pharma AG, Basel, Switzerland.

*D.T. Avery and A. Kane contributed equally to this paper; **E.K. Deenick and S.G. Tangye contributed equally to this paper; Correspondence to Stuart Tangye: s.tangye@garvan.org.au; Elissa Deenick: e.deenick@garvan.org.au.

and differentiation into long-lived memory and plasma cells (PCs; Goodnow et al., 2010; Tangye et al., 2013, 2015). These processes are controlled by signals received through the BCR, CD40, adhesion molecules, and receptors for cytokines and chemokines. A key effector downstream of these receptors is the phosphatidylinositide 3-kinase (PI3K) pathway (Okkenhaug and Vanhaesebroeck, 2003; Okkenhaug, 2013).

There are three classes of PI3K (Class IA, B; II; III) with Class IA PI3K being the predominant type involved in lymphocyte signaling (Okkenhaug and Vanhaesebroeck, 2003; Okkenhaug, 2013). Class IA PI3Ks (hereafter referred to as PI3K) are heterodimers, comprising a regulatory and catalytic subunit. Several isoforms of the regulatory (p85α, p85β, and p55) and catalytic (p110α, β, or δ) subunits have been identified. While p110α and β are ubiquitously expressed, p110δ is largely restricted to leukocytes (Okkenhaug and Vanhaesebroeck, 2003; Okkenhaug, 2013). PI3K is activated following engagement of the BCR or CD40, and its activation can be enhanced by coengagement of other receptors, such as CD19, BAFF-R and cyto/chemokine receptors (Ren et al., 1994; Aagaard-Tillery and Jelinek, 1996; Andjelic et al., 2000; Okkenhaug and Vanhaesebroeck, 2003; Okkenhaug, 2013). In B cells, PI3K becomes activated following p85-dependent recruitment to CD19 or the intracellular adaptor BCAP. This interaction represses the inhibitory function of p85, allowing activation of catalytic p110. PI3K converts membrane phosphatidylinositol-(4,5)-bisphosphate (PIP_2) to phosphatidylinositol-(3,4,5)-bisphosphate (PIP_3), which recruits TEC family kinases (ITK and BTK) and the serine/threonine kinase Akt to the inner plasma membrane of the cell. Anchoring of these kinases results in their activation, which then activate intracellular substrates and additional signaling pathways (Ras/MAPK, PKC, NFκB, and Akt/mTOR/FOXO1; Okkenhaug and Vanhaesebroeck, 2003; Okkenhaug, 2013). The action of PI3K is regulated by the lipid phosphatases PTEN (phosphatase and tensin homologue) and SHIP, which reduce PIP_3 levels by converting it to PIP_2 and phosphatidylinositol-(3,4)-bisphosphate, respectively (Okkenhaug and Vanhaesebroeck, 2003; Okkenhaug, 2013). Thus, production of PIP_3 by the balanced functions of PI3K and PTEN initiates activation of the major signaling pathways downstream of Ag, costimulatory and cytokine receptors in B cells that are critical for survival, growth, differentiation, and metabolism.

Analysis of genetically modified mice that lack p85α or p110δ, or express catalytically inactive p110δ, confirmed the importance of PI3K in B cell development and function. Compared with WT mice, these mutant mice have ∼50% fewer splenic follicular B cells, and a severe reduction in marginal zone (MZ) and B1 B cells (Fruman et al., 1999; Suzuki et al., 1999; Clayton et al., 2002; Jou et al., 2002; Okkenhaug et al., 2002; Srinivasan et al., 2009). More striking were the dramatically blunted Ab responses and generation of memory cells to T-dependent (TD) Ags, consistent with impaired GC formation in vivo and poor proliferation and survival of activated mutant B cells in vitro. PI3K also inhibits isotype switching by suppressing induction of *Aicda* (Omori et al., 2006; Dengler et al., 2008), encoding activation-induced cytidine deaminase (AID), or Ig germline transcripts (Dominguez-Sola et al., 2015; Sander et al., 2015), which are required for class switch recombination (CSR). These findings illustrate that PI3K-dependent signaling is required for B cell development, survival and eliciting TD Ab responses. Consistent with its role in restraining PI3K function, PTEN deficiency resulted in increased B cell numbers and serum IgM in vivo, and increased survival, proliferation, and Akt activation in vitro in response to BCR, CD40, or TLR signaling (Anzelon et al., 2003; Suzuki et al., 2003). Paradoxically, PTEN deficiency also resulted in poor GC and TD Ab responses and impaired CSR in vivo (Anzelon et al., 2003; Suzuki et al., 2003; Sander et al., 2015). Interestingly, conditional deletion of PI3K p110δ in $CD4^+$ T cells recapitulated the defect in humoral immune responses in germline-targeted *Pik3cd*-deficient mice (Rolf et al., 2010), suggesting an additional key B cell extrinsic function for PI3K signaling in regulating TD B cell differentiation. Thus, balanced signaling via PI3K is necessary for qualitatively and quantitatively robust humoral immune responses.

Recently, germline heterozygous gain-of-function (GOF) mutations in *PIK3CD*, encoding catalytic p110δ, have been identified to cause a primary immunodeficiency (Jou et al., 2006; Angulo et al., 2013; Crank et al., 2014; Kracker et al., 2014; Lucas et al., 2014a; Hartman et al., 2015; Elgizouli et al., 2016; Coulter et al., 2017). Affected individuals present with recurrent sinopulmonary infections, lymphadenopathy, splenomegaly, and viremia due to uncontrolled infection by human herpes viruses. While these patients have normal/elevated levels of IgM, variable levels of IgG and low/normal levels of IgA, Ag-specific Ab titres against protein- and polysaccharide-containing vaccines are consistently low (Jou et al., 2006; Angulo et al., 2013; Crank et al., 2014; Deau et al., 2014; Kracker et al., 2014; Lucas et al., 2014a; Hartman et al., 2015; Elgizouli et al., 2016; Coulter et al., 2017). Thus, *PIK3CD* GOF mutations underlie a novel human immunodysregulatory disorder thereby highlighting the complex regulation of PI3K signaling. Despite this, the mechanism(s) underlying the cellular defects due to *PIK3CD* GOF mutations remains unknown. To delineate requirements for p110δ in B cell function, we have now examined B cell development and differentiation in a large cohort of individuals with *PIK3CD* GOF mutations, as well as a corresponding CRISPR/Cas9 gene-edited mouse model.

Results

Gain of function mutations in *PIK3CD* impede human B cell development and differentiation in vivo

Ex vivo analysis of B cells from *PIK3CD* GOF patients revealed elevated levels of phosphorylated ribosomal S6 protein (pS6), which is downstream of mTOR, compared with B cells from healthy donors, confirming hyperactive PI3K signaling (Fig. S1 A). The key clinical features of patients with *PIK3CD* GOF mutations (recurrent respiratory tract infections, increased serum IgM, concomitant hypogammaglobulinemia, impaired humoral immune responses following infection or vaccination; Angulo et al., 2013; Lucas et al., 2014a; Coulter et al., 2017) point to a defect in B cell development and/or function. To investigate this, we assessed the proportions and phenotype of distinct B cell subsets in a large cohort of affected individuals. Our cohort comprised 39 patients from 27 different families. The mean age of the *PIK3CD* GOF patients was 18 yr (range: 6–65 yr), and 29/39 (∼74%) carried the common E1021K mutation. Analysis of the B cell compartment

revealed comparable frequencies of CD20$^+$ B cells in *PIK3CD* GOF patients and healthy controls (Fig. 1 A; controls: 9.8 ± 0.8%, n = 45; patients: 11.5 ± 1.3%, n = 39; mean ± SEM). However, delineation of circulating B cells into populations of transitional, naive, and memory B cell subsets (Cuss et al., 2006; Avery et al., 2010; Suryani et al., 2010) revealed marked differences. Specifically, the proportions of transitional B cells were significantly increased (controls: 13.5 ± 1.0%, n = 60; patients: 53.4 ± 3.1%, n = 38), while those of naive (controls: 62.9 ± 1.2%, patients: 38.7 ± 2.8%) and memory (controls: 21.5 ± 1.8%, patients: 6.3 ± 0.7%) B cells were significantly reduced in *PIK3CD* GOF patients compared with healthy controls (Fig. 1 B). To extend the analysis of defects in B cell differentiation, we also determined proportions of class-switched memory B cells. In healthy donors, ∼20–25% of memory B cells express IgG or IgA (Avery et al., 2010; Fig. 1 C). In contrast, on average <10% of memory B cells in *PIK3CD* GOF patients expressed IgG or IgA (Fig. 1 C). Thus, *PIK3CD* GOF mutations not only compromised the ability of affected individuals to generate a normal memory B cell pool, but also impaired isotype switching, yielding fewer class switched B cells.

The proportion of transitional B cells in peripheral blood of healthy donors is highest at birth and rapidly declines within the first 5 yr, before continuing to decline at a slower rate over subsequent years (Sims et al., 2005; Cuss et al., 2006; Morbach et al., 2010). Conversely, memory B cells are absent from umbilical cord blood, progressively increase over the first two decades of life, and then plateau after ∼25 yr of age (Agematsu et al., 1997; Morbach et al., 2010). As ∼70% of our cohort of individuals with *PIK3CD* GOF mutations were aged between 5 and 20 yr, it was possible that the skewing in composition of the B cell compartment reflected differences in the mean age of the patient cohort compared with that of healthy controls (18.0 vs. 28.5 yr). To investigate this, we determined proportions of B cell subsets according to the age of individual donors and patients. This analysis indeed confirmed the reciprocal relationship between transitional and memory B cells with age in both healthy donors and *PIK3CD* GOF mutant patients (Fig. 1 D). However, it is clear that the average proportion of transitional B cells in the patients exceeded those in controls, while those of memory B cells in healthy donors were greater than in the patients, irrespective of age (Fig. 1 D). Similar findings were made when class switching in the memory B cell compartment was analyzed with respect to age (not shown). Thus, *PIK3CD* GOF mutations profoundly alter B cell development and differentiation.

PIK3CD GOF mutations result in the accumulation of early transitional B cells in the periphery

Analysis of the expanded population of transitional B cells in individuals with *PIK3CD* GOF mutations revealed increased surface expression of CD10 compared with corresponding transitional B cells from healthy donors (see contour plots in Fig. 1 B). As CD10 decreases on human progenitor cells as they progress through successive stages of B cell development (Uckun, 1990), we questioned whether transitional B cells in *PIK3CD* GOF patients were developmentally less mature than those detected in healthy donors. To address this, we determined expression of a suite of molecules that have previously been established to increase or decrease as transitional B cells mature into naive B cells, which then differentiate into memory B cells (Sims et al., 2005; Cuss et al., 2006; Suryani et al., 2010). Consistent with previous studies, CD5 and CD38 were highly expressed on transitional B cells, and then greatly down-regulated on naive and memory B cells (Sims et al., 2005; Cuss et al., 2006; Suryani et al., 2010). IgM is also reduced as transitional B cells mature into naive B cells (not shown). In contrast, levels of CD44 and Bcl-2 increase as transitional B cells develop into naive B cells and subsequently differentiate into memory B cells. Levels of other surface receptors such as CD21, CD23, CCR7, CXCR4, and CXCR5 also increase as transitional B cells develop into naive B cells, but are then down-regulated during naive→memory differentiation (Fig. 2).

Although the patterns of expression of these molecules by B cell subsets in *PIK3CD* GOF patients mirrored those of B cells from healthy controls, there were marked differences in the absolute levels of expression. Thus, CD5 and CD38 were approximately threefold higher on transitional and naive B cells from *PIK3CD* GOF patients than on controls, and remained detectable on *PIK3CD* GOF memory B cells (Fig. 2, A and B). IgM also remained greatly increased (greater than threefold) on *PIK3CD* GOF transitional and naive B cells (not shown). CD21, CD44, Bcl-2, CCR7, CXCR4, and CXCR5 were up to threefold lower on B cell subsets from *PIK3CD* GOF patients compared with controls (Fig. 2 C, E, G–I). CD23 was also reduced on *PIK3CD* GOF transitional and naive B cells, and failed to be down-regulated on memory B cells (Fig. 2 D). Since PI3K is activated downstream of CD19, and CD81 forms a complex with CD19 and other B cell coreceptors (Carter and Barrington, 2004), we also assessed expression of these molecules. CD19 was significantly reduced on naive B cells, while CD81 was significantly increased on transitional B cells, from *PIK3CD* GOF patients compared with controls (Fig. 2 F; not shown).

There are at least two subsets of transitional B cells detectable in human peripheral blood (Anolik et al., 2007; Palanichamy et al., 2009; Suryani et al., 2010). Our previous studies delineated CD21^{lo} and CD21^{hi} subsets of transitional B cells, with the CD21^{lo} subset being less mature and a precursor of the CD21^{hi} subset (Suryani et al., 2010). The above phenotyping data revealed that the majority of transitional B cells in *PIK3CD* GOF patients corresponded to the CD21^{lo} subset. They also suggested that CD20$^+$CD10$^-$CD27$^-$ B cells in *PIK3CD* GOF patients were less mature than corresponding naive B cells from healthy donors, since the former exhibited a phenotype more similar to that of normal transitional rather than naive B cells. To further investigate these B cell defects, we determined expression levels of genes differentially expressed during peripheral B cell development. *LEF1* and *DTX1* are more highly expressed in CD21^{lo} than in CD21^{hi} transitional B cells (Suryani et al., 2010). Quantitative PCR (qPCR) analysis revealed *DTX1* was expressed at 5- and 10-fold–higher levels in transitional and naive B cells, respectively, from *PIK3CD* GOF patients than in these cells from health donors (Fig. S1 B). Similarly, while *LEF1* is expressed in transitional B cells and extinguished in naive B cells from healthy donors, it continued to be expressed in *PIK3CD* GOF naive B cells (Fig. S1 B). Thus, the circulating B cell compartment of patients with *PIK3CD* GOF mutations is enriched for cells at early stages of B cell development.

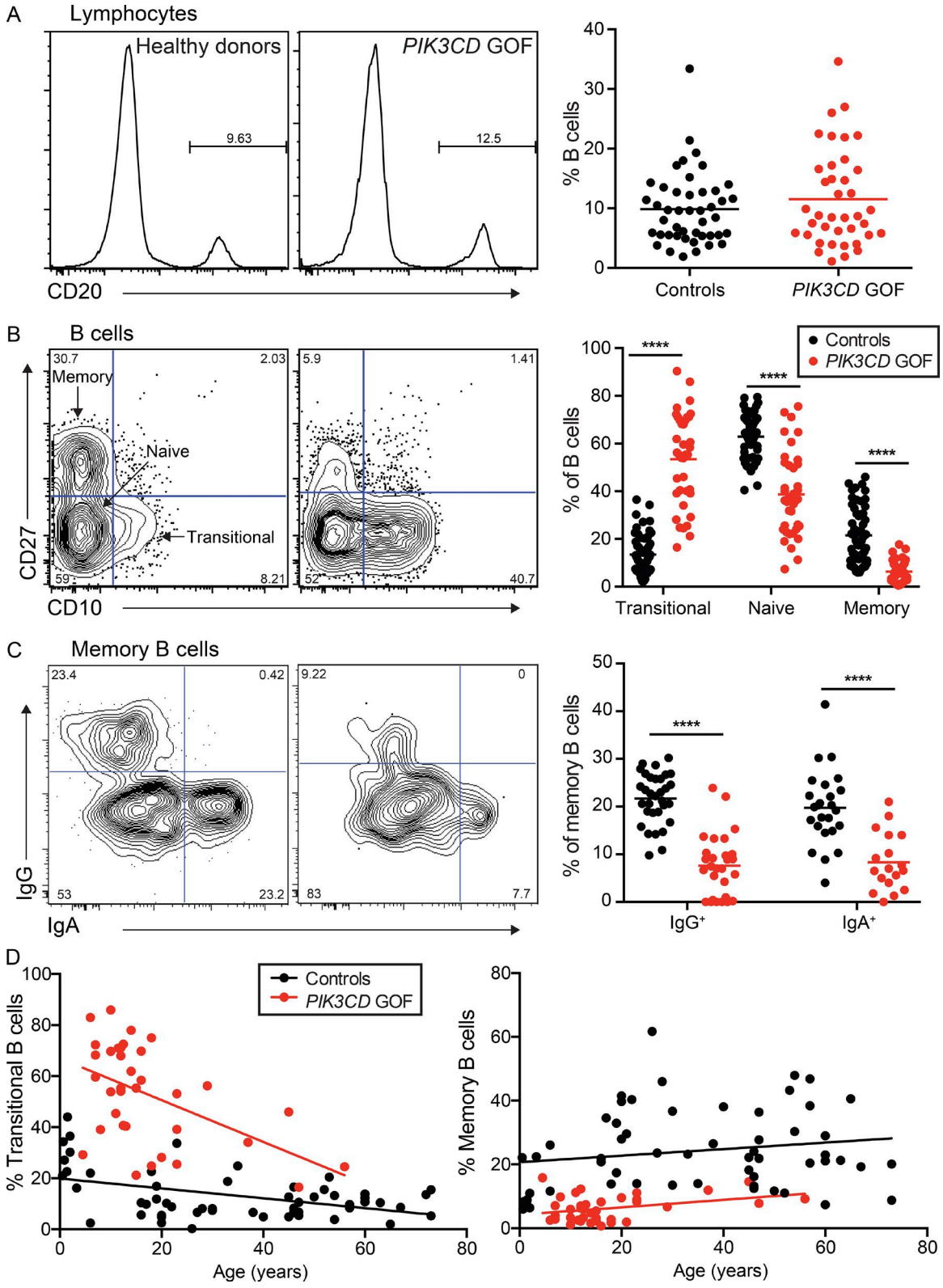

Figure 1. **GOF mutations in *PIK3CD* arrest peripheral B cell development and differentiation.** PBMCs from healthy donors (n = 45–60) and patients with *PIK3CD* GOF mutations (n = 21–39) were labeled with mAbs against CD20, CD10, CD27, IgG, or IgA. The proportions of **(A)** B ($CD20^+$) cells within the lymphocyte gate, **(B)** transitional, naive, and memory cells within the B cell population, and **(C)** IgG^+ and IgA^+ cells within the memory population were determined by flow cytometry. Histogram and contour plots are representative of healthy donors or *PIK3CD* GOF patients. Each symbol in the summary graphs corresponds to an individual donor or patient; horizontal bars represent the mean. Significant differences were determined by unpaired Student's t tests. ****, $P < 0.0001$. **(D)** Proportions of transitional (left panel) and memory (right panel) B cells in healthy donors (black) and *PIK3CD* GOF patients (red) were determined as a function of age.

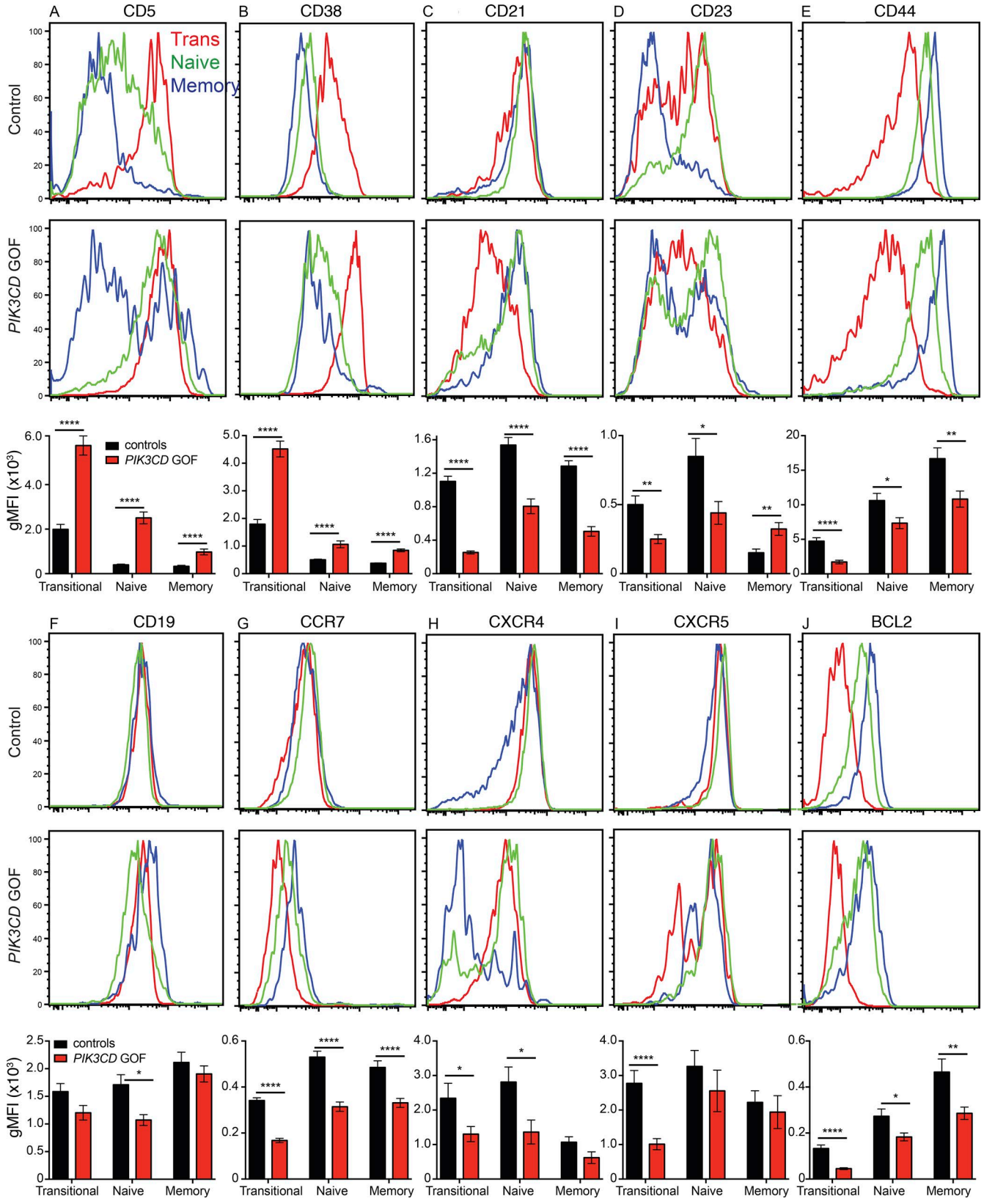

Figure 2. **Peripheral B cells in *PIK3CD* GOF patients have an immature phenotype.** Expression of **(A)** CD5, **(B)** CD38, **(C)** CD21, **(D)** CD23, **(E)** CD44, **(F)** CD19, **(G)** CCR7, **(H)** CXCR4, **(I)** CXCR5, or **(J)** BCL2 was determined on transitional, naive, and memory B cells in peripheral blood of healthy donors or patients with *PIK3CD* GOF mutations (n = 6–30). Histogram plots are representative of healthy donors (upper panels) or *PIK3CD* GOF patients (lower panels). The bar graphs depict the geometric mean fluorescence intensity (± SEM) of each indicated molecule. Significant differences were determined by unpaired Student's t tests. *, P < 0.05; **, P < 0.01; ****, P < 0.0001.

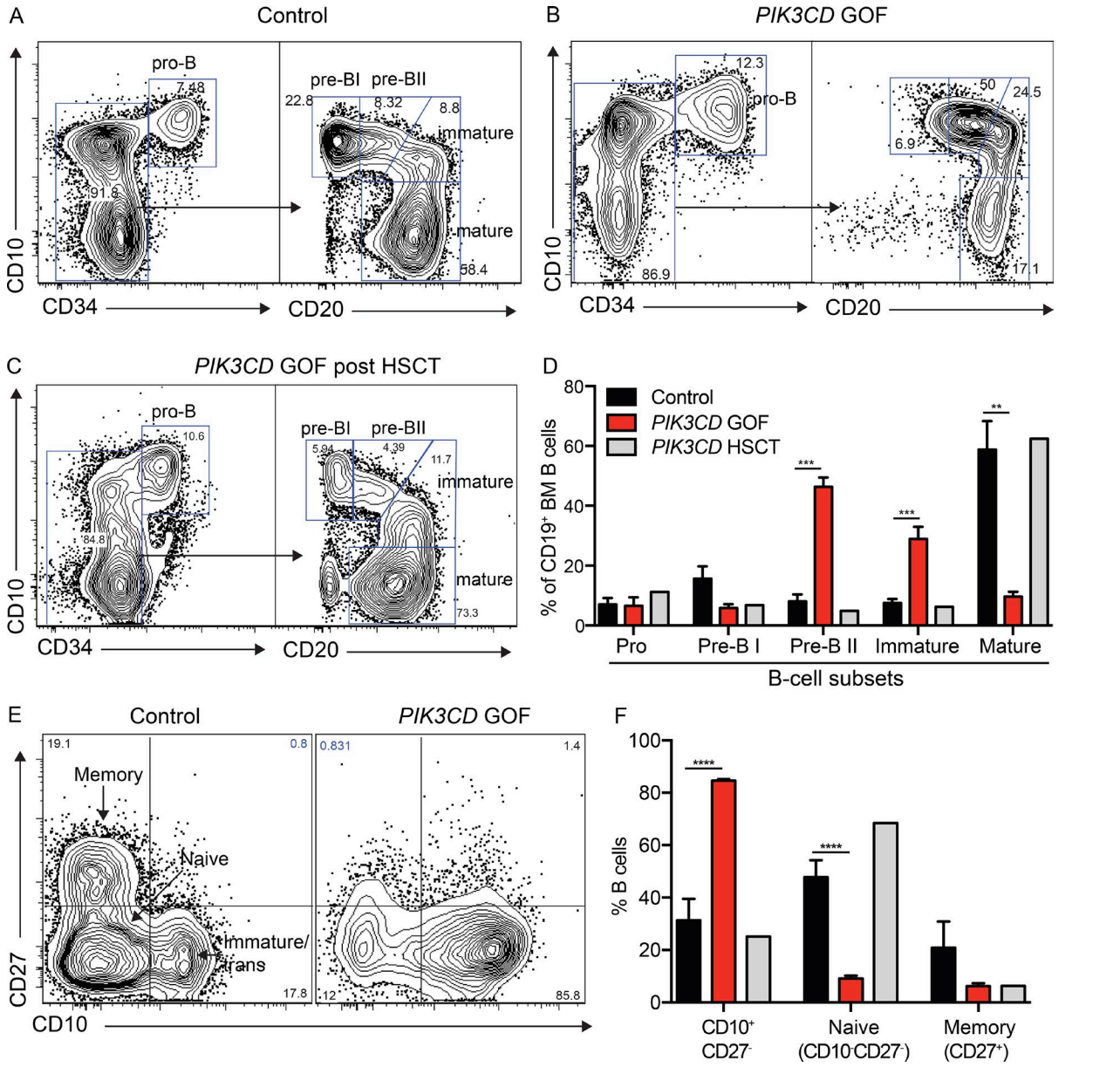

Figure 3. ***PIK3CD* GOF mutations block B cell development in the bone marrow at the pre-BII stage.** BM aspirates from healthy donors (n = 6), patients with *PIK3CD* GOF mutations (n = 3), or one patient following hematopoietic stem cell transplant were labeled with mAbs against CD34, CD19, CD20, CD10, IgM, and CD27. Proportions of pro-B ($CD19^+CD34^+CD10^+CD20^-IgM^-$), pre-BI ($CD19^+CD34^-CD10^+CD20^-IgM^-$), pre-BII ($CD19^+CD34^-CD10^+CD20^{dim}IgM^-$), immature ($CD19^+CD34CD10^+CD20^+IgM^+$), and recirculating mature ($CD19^+CD34^-CD10^-CD20^+$) B cells were determined. **(A–C)** Contour plots in show CD34 versus CD10 staining to identify pro-B cells, which were then further analyzed for pre-BI, pre-BII, immature, and recirculating mature according to differential expression of CD20 and CD10. **(D)** Mean ± SEM of the different subsets of B cells in the BM. **(E)** Representative contour plots showing CD10 versus CD27 staining on $CD20^+$ B cells, and **(F)** mean ± SEM of $CD10^+CD27^-$, naive ($CD20^+CD10^-CD27^-$) and memory ($CD20^+CD27^+$) B cells in the BM. Significant differences were determined by Student's t test. **, P < 0.01; ***, P < 0.001; ****, P < 0.0001.

PIK3CD GOF mutations cause aberrant B cell development in the bone marrow

B cell development occurs in the BM, where hematopoietic stem cells undergo progressive steps to yield pro-B, pre-B, and immature B cells before being exported to the periphery as transitional cells (Uckun, 1990). To further explore the nature of the defect in B cell development observed in the peripheral blood, we quantified the proportions of pro-B ($CD19^+CD34^+CD10^+CD20^-IgM^-$), preBI ($CD19^+CD34^-CD10^+CD20^-IgM^-$), preBII ($CD19^+CD34^-CD10^+CD20^{dim}IgM^-$), immature ($CD19^+CD34^-CD10^+CD20^+IgM^+$), and mature ($CD19^+CD34^-CD10^-CD20^+$) B cells in the BM (Uckun, 1990; van Zelm et al., 2005) of *PIK3CD* GOF patients. Proportions of pro-B and preBI cells in controls and patients were similar (Fig. 3, A, B, and D). However, compared with BM from healthy donors, we found significantly increased proportions of preBII and immature B cells, and marked reductions in mature recirculating B cells ($CD19^+CD20^+CD10^-$) in BM from *PIK3CD* GOF patients (Fig. 3, A, B, and D).

To extend the findings from analysis of peripheral blood, we enumerated naive and memory B cells in the BM. When $CD19^+$ B

cells were defined according to differential expression of CD10 and CD27, there were significant increases in $CD10^+$ B cells and significant decreases in naive ($CD10^-CD27^-$) B cells in BM from *PIK3CD* GOF patients compared with healthy controls (Fig. 3, E and F). There was also a trend toward decreased proportions of memory ($CD10^-CD27^+$) B cells in *PIK3CD* GOF BM compared with healthy controls (6.2 ± 1.2 vs. 20.8 ± 10.0; Fig. 3, E and F). Upon analysis of BM from one *PIK3CD* GOF patient who had undergone hematopoietic stem cell transplant, these defects in B cell development were corrected (Fig. 3, C, D, and F). Thus, the peripheral accumulation of immature transitional B cells in patients with *PIK3CD* GOF mutations results from perturbed B cell development in the BM, with a block in the ability of pro-B, pre-B, and immature B cells to progress to the subsequent stages of B cell maturation. These defects are likely B cell intrinsic and can be corrected by hematopoietic stem cell transplant.

PIK3CD mutations selectively compromise the differentiation of B cells into class switched Ig secreting plasmablasts

Impaired humoral immune responses following natural infection or immunization characterized by reduced levels of total and Ag-specific serum Ig are hallmarks of the immunodeficiency associated with *PIK3CD* GOF mutations (Angulo et al., 2013; Lucas et al., 2014a; Coulter et al., 2017). Data from mice indicated that germline targeting of *Pik3cd*, or conditional loss of *Pten* from B cells, compromised humoral immunity in response to TD and T-independent (TI) Ags (Clayton et al., 2002; Jou et al., 2002; Okkenhaug et al., 2002; Suzuki et al., 2003; Omori et al., 2006). Thus, regulated function of PI3K signaling is critical for generating robust and long-lived Ab responses.

To determine the impact of *PIK3CD* GOF mutations on the function of human B cells, transitional and naive B cells were sorted from the peripheral blood of healthy donors and patients and subjected to in vitro culture. Proliferation of naive *PIK3CD* GOF B cells, as determined by dilution of CFSE, in response to mimics of TD (e.g., CD40L ± cytokines) and TI (e.g., BCR and TLR engagement) stimulation was comparable to, or slightly greater than, that of naive B cells from healthy controls (Fig. S1 C). Thus, the paucity of class switched memory B cells and impaired humoral immune responses in *PIK3CD* GOF patients cannot be explained by a proliferation defect in naive B cells.

Next, we assessed differentiation of naive B cells into plasmablasts upon stimulation with CD40L and IL-21 for 5 d. This combination of stimuli is not only a potent means of inducing human B cell proliferation and differentiation (Moens and Tangye, 2014), but both CD40L (Ren et al., 1994; Aagaard-Tillery and Jelinek, 1996; Andjelic et al., 2000) and IL-21 (Ostiguy et al., 2007; Zeng et al., 2007) individually activate PI3K. Indeed, CD40-induced proliferation and IL-21–induced up-regulation of CD86 are reduced or abolished in murine *Pik3cd* and *Pik3r1* mutant B cells (Fruman et al., 1999; Suzuki et al., 1999; Clayton et al., 2002; Jou et al., 2002; Okkenhaug et al., 2002; Attridge et al., 2014). Under these culture conditions, comparable proportions (~3–8%) of naive B cells from healthy controls or patients up-regulated expression of CD38 and CD27 and down-regulated CD20 ($CD38^{hi}CD27^{hi}CD20^{lo}$), thereby acquiring a plasmablast phenotype (Avery et al., 2005; Fig. 4, A and B). Consistent with this, induction of *PRDM1* mRNA (encoding Blimp-1; Fig. 4 C) as well as of Blimp-1 protein in plasmablasts (Fig. 4 D) was intact for patients' naive B cells. As AID contributes to the B cell response by inducing CSR (Durandy et al., 2007), we determined induction of *AICDA* mRNA in activated naive B cells. While *AICDA* was induced in *PIK3CD* GOF naive B cells by CD40L/IL-21, it tended to be less than levels observed in naive B cells from healthy donors (Fig. 4 E).

To explore B cell differentiation in vitro in more detail, we determined the quality of the plasmablast response. Intracellular staining revealed that ~60% of plasmablasts generated from normal naive B cells expressed IgG, with the remaining expressing IgM or IgA (~20% of each; Fig. 4, F and G). Strikingly, the majority of plasmablasts generated from *PIK3CD* GOF naive B cells continued to express IgM, and only ~10% had undergone CSR to IgG (Fig. 4, F and G). Remarkably, class switching by *PIK3CD* GOF naive B cells to IgA was intact (Fig. 4, F and G). Analysis of Ig secretion by in vitro stimulated naive B cells confirmed these findings, with a sharp reduction (~10-fold) in levels of IgG, but normal levels of IgM and IgA (Fig. 4 H). The poor secretion of IgG by *PIK3CD* GOF naive B cells did not reflect delayed kinetics of differentiation into IgG-secreting cells, because this defect was also noted after 7 d of culture (Fig. 4 H).

We also tested the functionality of transitional cells, as these cells dominate the B cell population in *PIK3CD* GOF patients (Fig. 1 B). Similar to naive cells, induction of *PRDM1* mRNA (Fig. 4 C) and production of IgM (Fig. 4 I) by *PIK3CD* GOF transitional B cells in response to CD40L/IL-21 stimulation was intact. *AICDA* expression was also induced in activated *PIK3CD* GOF transitional B cells and modestly reduced compared with control transitional B cells (Fig. 4 E). Despite these findings, *PIK3CD* GOF transitional B cells were unable to produce normal amounts of IgG (>50-fold reduction compared with controls after 5 and 7 d of in vitro culture; Fig. 4 I). Notably, *PIK3CD* GOF transitional B cells also exhibited a significant defect in switching to IgA at both time points examined (Fig. 4 I). Collectively, these findings establish that while hyperactive PI3K signaling has no effect on proliferation of human B cells, nor their initial differentiation into Ig-secreting cells, it impairs the ability of naive B cells to undergo class switching to IgG and of transitional B cells to produce IgG and IgA.

A gene set associated with plasmablast differentiation is poorly induced in *PIK3CD* GOF transitional B cells

To explore molecular defects underlying impaired differentiation of *PIK3CD* GOF B cells, we determined gene expression profiles of transitional B cell subsets from healthy donors and *PIK3CD* GOF patients following in vitro culture with CD40L alone or together with IL-21. Modulation of key genes involved in IL-21–mediated differentiation of human B cells into plasmablasts was largely unaffected by *PIK3CD* GOF mutations. Specifically, *PRDM1, XBP1, IRF4, MZB1,* and *IL10* were induced, while *CCR7* and *BACH2* were down-regulated in control and *PIK3CD* GOF transitional B cells following culture with CD40L/IL-21 compared with cells cultured with CD40L alone (Fig. 5 A). In contrast, *PAX5* was down-regulated in control, but less so in *PIK3CD* GOF transitional B cells (Fig. 5 A; confirmed by qPCR, not shown). Unbiased analysis and comparison of transcriptomes from CD40L/IL-21–stimu-

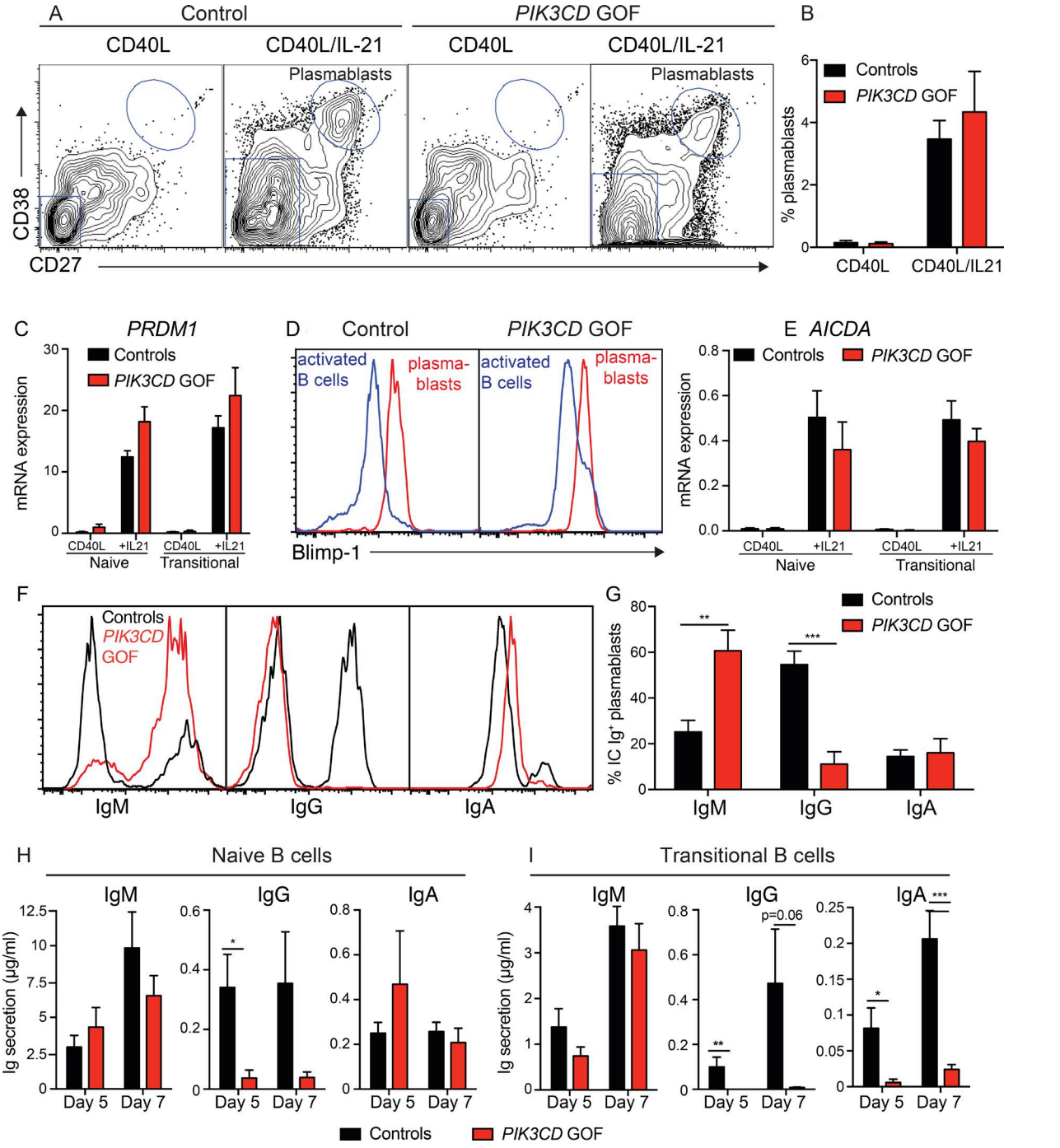

Figure 4. **Intact differentiation to plasmablasts but impaired class switching in *PIK3CD* GOF naive and transitional B cells. (A–G)** Naive and/or transitional B cells from healthy donors or *PIK3CD* GOF patients were cultured for 5 d with CD40L alone or together with IL-21. **(A and B)** Proportions of $CD38^{hi}CD27^{hi}$ plasmablasts generated from naive B cells were determined by flow cytometry (n = 7–8). **(C and D)** Expression of Blimp-1 was determined by (C) qPCR in naive and transitional B cells cultured with CD40L or CD40L/IL-21 (n = 5) and (D) flow cytometry of activated B cell blasts ($CD27^{-}CD38^{-/lo}$) and plasmablasts generated from naive B cells cultured with CD40L or CD40L/IL-21 (n = 4–5). **(E)** Expression of *AICDA* was determined by qPCR in naive and transitional B cells cultured with CD40L or CD40L/IL-21 (n = 5). **(F and G)** Expression of intracellular IgM, IgG, and IgA by plasmablasts was determined by flow cytometry (n = 5–6). The FACS plots in A, D, and F are representative of cultured naive B cells from healthy donors or *PIK3CD* GOF patients; the graphs in B, C, E, and G depict the mean ± SEM of independent experiments using naive B cells from different donors and patients. **(H and I)** Sort-purified naive (H; n = 9–12) and transitional (I; n = 11–14) B cells from healthy donors or *PIK3CD* GOF patients were cultured for 5 or 7 d with CD40L and IL-21. Ig secretion was then determined. Values represent the mean ± SEM. Significant differences were determined by Student's t tests. *, P < 0.05; **, P < 0.01; ***, P < 0.001.

lated control and *PIK3CD* GOF transitional B cells identified 346 differentially expressed genes (DEGs; absolute fold change >1.5, false discovery rate [FDR] <0.05; Fig. S2 A). Non-negative matrix factorization (NMF; Brunet et al., 2004; Kim and Park, 2007) was performed on this set of DEGs to identify the key molecular drivers underlying differences in the gene expression profiles of

normal and *PIK3CD* GOF activated transitional B cells (Fig. 5 B). Among the driver genes highly expressed by activated *PIK3CD* GOF relative to normal transitional B cells were *SIGLEC6*, which is expressed on human B cells and inhibits their proliferation and differentiation (Patel et al., 1999; Kardava et al., 2011), *MPEG1*, *KMO*, the CD20-like gene *MS4A7* (Fig. 5 B), as well as *MSA4A1* (CD20), *CD72*, *CD22*, *CD84*, *FCGR2C*, and *CD24* (Fig. S2 A), which are all typically down-regulated as B cells differentiate into PCs (Ellyard et al., 2004; Avery et al., 2005; Jourdan et al., 2011). Additionally, *CD27* and *SLAMF7*, which are highly expressed by primary human PCs (Jung et al., 2000; Ellyard et al., 2004; Good et al., 2009), were up-regulated in normal, but not *PIK3CD* GOF, transitional B cells following in vitro stimulation with CD40L/IL-21 compared with culture with CD40L alone (Fig. 5 B).

We adopted several approaches to confirm these findings relating to differential gene expression in activated control and *PIK3CD* GOF transitional B cells. First, to ascertain the biological and physiological relevance of the pattern of differentially expressed genes between *PIK3CD* GOF and control transitional B cells, we performed RNA-seq on B cell subsets isolated from human tonsils. Analysis of this dataset clearly revealed that the genes identified from the microarrays to be highly expressed in activated *PIK3CD* GOF transitional B cells, but down-regulated in control transitional B cells, are characteristic of resting naive and memory tonsil B cells (i.e., *KMO*, *MPEG1*, *MS4A7*, *PTPRJ*, *RAP GAP12*, and *SIGLEC6*; Fig. S2 B). In contrast, genes up-regulated in normal, but not *PIK3CD* GOF, transitional B cells following in vitro culture with CD40L/IL-21 were expressed at the highest levels in primary human PCs (i.e., *CD27*, *SLAMF7*, *ZNF251*, *SLC29A1*, *MYO1D*, and *BEX5*; Fig. S2 C; Jung et al., 2000; Ellyard et al., 2004; Good et al., 2009). The RNA-Seq data were next confirmed by qPCR analysis of gene expression in tonsil naive, memory, GC cells, and PCs isolated from a second cohort of individuals undergoing tonsillectomy. This established that *KMO*, *MS4A7*, *PTP RJ*, *RAP1GAP2*, and *SIGLEC6* are more highly expressed in naive and/or memory B cells, while *SLAMF7*, *ZNF215*, *GPR15*, *MYO1D*, and *BEX5* are highly expressed in PCs (Fig. 5, C and D). Flow cytometric analysis of tonsil B cell subsets confirmed increased expression of Siglec-6 on memory B cells, and reduced expression on PCs (Fig. S2 D), but increased expression of CRACC (SLA MF7) and CD27 on PCs compared with naive, memory and GC B cells (Fig. S2, E and F). Consistent with this, Siglec-6 was expressed at higher levels on in vitro–activated B cells compared with plasmablasts following culture with CD40L/IL-21, while CRACC and CD27 were induced on plasmablasts generated in vitro from naive B cells in the same cultures (Fig. S2 G). Third, gene set enrichment analysis indicated that activated *PIK3CD* GOF transitional B cells exhibit gene expression profiles that are more consistent with naive or memory B cells rather than PCs, which, akin to the phenotype of cultured *PIK3CD* GOF transitional B cells, contrasts with activated transitional B cells from healthy controls (Fig. S2 H). Fourth, we directly measured the ability of *PIK3CD* GOF transitional B cells to differentiate into plasmablasts in vitro. Strikingly, these B cells failed to give rise to $CD38^{hi}CD27^{hi}$ plasmablasts following culture with CD40L/IL-21 (Fig. 5 E). This starkly contrasted the response of transitional B cells from healthy donors (Fig. 5 E), as well as naive B cells from healthy donors and *PIK3CD* GOF patients (Fig. 4, A and B). To extend these observations, and validate the differential expression of several of the genes identified by microarray, qPCR was performed using cDNA from activated control and *PIK3CD* GOF transitional B cells. This revealed markedly increased expression of *KMO*, *MS4A7*, *PTPRJ*, and *SIGLEC6*, but decreased expression of *SLAMF7* and *MYO1D* by in vitro CD40L/IL-21–activated *PIK3CD* GOF transitional B cells compared with controls (Fig. 5 F). These data underscore the findings from the microarray, phenotypic, and functional analysis of *PIK3CD* GOF B cells and collectively establish that induction of a plasmablast transcriptional signature is compromised in *PIK3CD* GOF transitional B cells, even though these cells can exhibit some features of early differentiation to the Ig-secreting cell lineage.

Development of a mouse model of *Pik3cd* GOF

To further explore how PI3K overactivation alters B cell development and function we used CRISPR/Cas9 gene editing to introduce a heterozygous E1020K mutation in *Pik3cd* in the germline of C57BL/6 mice. This is the orthologue of the most common mutation found in the human *PIK3CD* gene (E1021K). We assessed PI3K activity in these animals by staining splenocytes for phosphorylated Akt (T308 and S473). B cells in these mice displayed significant increases in basal levels of phosphorylation of both T308 and S473 (Fig. 6 A and Fig. S3 A). pS6 protein was similarly increased in B cells of $Pik3cd^{E1020K}$ GOF mice compared with WT mice (Fig. 6 A and Fig. S3 A), consistent with our observations of *PIK3CD* GOF human B cells (Fig. S1 A). Mice homozygous for the $Pik3cd^{E1020K}$ GOF mutation showed even greater activation of these signaling pathways (Fig. 6 A), indicating a dose-dependent effect of the activating mutation. Importantly, similar to human lymphocytes (Rao et al., 2017), increased levels of pAkt and pS6 in $Pik3cd^{E1020K}$ GOF murine B cells could be reduced by preincubation with leniolisib, a p110δ-specific inhibitor (Fig. S3, A and B; Hoegenauer et al., 2017) demonstrating that heightened activation of these signaling components was PI3K dependent.

$Pik3cd^{E1020K}$ GOF mice allowed us to investigate the effect of overactive PI3K on B cell development in multiple lymphoid organs without any complications of ongoing infections or prior/current treatments. Analysis of BM revealed an increase in pro-B cells and a decrease in mature recirculating IgD^{hi} cells in $Pik3cd^{E1020K}$ GOF mice compared with WT controls (Fig. 6 B). Analysis of mixed BM chimeras demonstrated that these effects on B cell development in the BM were cell intrinsic (not shown).

Given the decrease in mature B cells in the BM we also examined B cells in the periphery. Spleens of $Pik3cd^{E1020K}$ GOF mice had increased cellularity over WT spleens, which was at least in part due to an increase in total numbers of B cells (data not shown). Staining with CD93 allowed us to identify transitional B cells. This revealed an overall increase in absolute number of transitional B cells (data not shown), which was due to an almost threefold increase in the number of T1 B cells (Fig. 6 C). Interestingly we observed a significant down-regulation of IgM on T1 B cells from $Pik3cd^{E1020K}$ GOF mice compared with those from WT controls (Fig. 6 C). We also noted an increased number of cells that down-regulated IgM within the $CD23^{+}$ T2/T3 gate, consistent with increased numbers of anergic T3 cells (Fig. 6 C). The

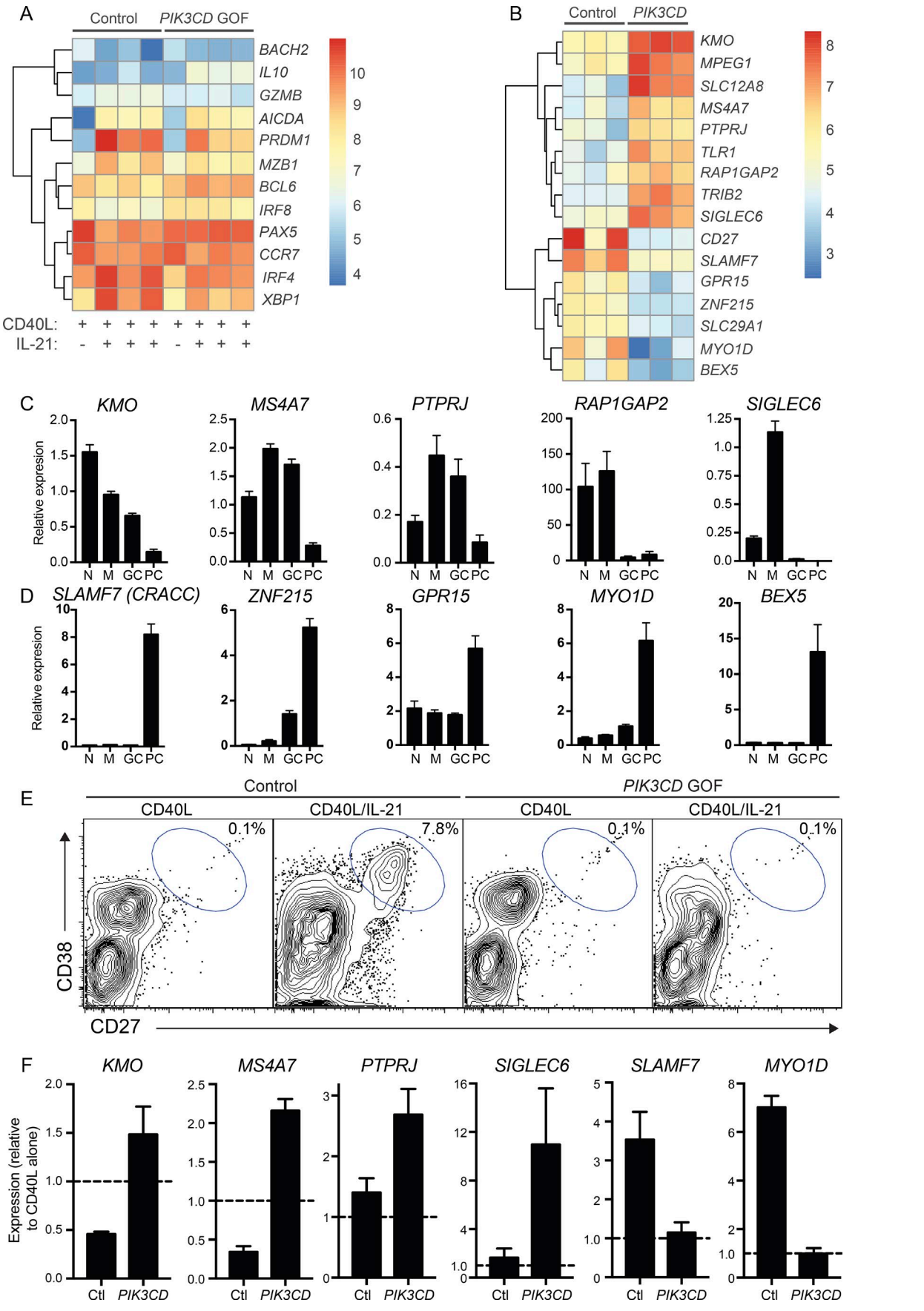
A
Control
PIK3CD GOF
BACH2
IL10
GZMB
AICDA
PRDM1
MZB1
BCL6
IRF8
PAX5
CCR7
IRF4
XBP1
CD40L:
IL-21:
B
Control
PIK3CD
KMO
MPEG1
SLC12A8
MS4A7
PTPRJ
TLR1
RAP1GAP2
TRIB2
SIGLEC6
CD27
SLAMF7
GPR15
ZNF215
SLC29A1
MYO1D
BEX5
C
KMO
MS4A7
PTPRJ
RAP1GAP2
SIGLEC6
Relative expresion
N M GC PC
D
SLAMF7 (CRACC)
ZNF215
GPR15
MYO1D
BEX5
E
Control
PIK3CD GOF
CD40L
CD40L/IL-21
0.1%
7.8%
CD38
CD27
F
KMO
MS4A7
PTPRJ
SIGLEC6
SLAMF7
MYO1D
Expression (relative to CD40L alone)
Ctl
PIK3CD

mature ($CD93^-$) B cell pool in *Pik3cd*^{E1020K} GOF mice was also expanded, with a striking increase in MZ cells. In contrast follicular B cells were only slightly increased (Fig. 6 D). We also observed an increase in B1 cells in the spleen, particularly B1a cells (Fig. 6 E). Mixed BM chimeras established that these changes in B cell maturation within the spleen were cell intrinsic (not shown). Analysis of B cell populations in the circulation revealed comparable proportions of total B cells in *Pik3cd*^{E1020K} GOF mice, but increased proportions of B1 and transitional B cells and decreased proportions of mature B cells compared with WT mice (Fig. S3, C–F). This is consistent with our observations of spleens from *Pik3cd*^{E1020K} GOF mice (Fig. 6) and the blood of *PIK3CD* GOF patients (Figs. 1 and 2).

Pik3cd GOF B cells have impaired Ig class switching in vitro

Analysis of human B cells showed decreased class switched memory cells in vivo and decreased production of switched plasmablasts and secretion of IgG in vitro. To determine whether PI3K overactivation lead to a decrease in switching to distinct IgG subclasses in response to different stimuli, we sorted follicular B cells from the spleens of WT or *Pik3cd*^{E1020K} GOF mice and stimulated them with anti-CD40 + IL-4, LPS, or LPS + TGF-β to induce CSR to IgG1, IgG2b, or IgG3, respectively (Hodgkin et al., 1996; Hasbold et al., 1998, 2004; Deenick et al., 1999). After 4 d, 50% fewer *Pik3cd*^{E1020K} GOF follicular B cells were positive for these switched isotypes following culture under the three different conditions compared with B cells from WT mice (Fig. 7, A–C). This was not due to switching to alternative isotypes, as we saw no increases in expression of other IgG subclasses or IgA (data not shown).

As class switching is division linked (Hodgkin et al., 1996; Hasbold et al., 1998, 2004; Deenick et al., 1999), we also labeled B cells with CFSE to determine the percentage of switched cells in each division. The proportion of WT B cells undergoing CSR sharply increased after three divisions, and this continued to increase with subsequent divisions (Fig. 7, A–C), consistent with previous findings (Hodgkin et al., 1996; Hasbold et al., 1998, 2004; Deenick et al., 1999). *Pik3cd*^{E1020K} GOF B cells also underwent CSR in a division-linked manner, however the percentage of switched cells in each division remained approximately half of that seen for WT cells (Fig. 7, A–C). Thus, similar to our observations for human B cells, activating mutations in PI3K p110δ impede Ig class switching, but not proliferation, by murine B cells.

Analysis of *Pik3cd* GOF B cell responses in vivo revealed decreased Ig class switching but normal expansion and affinity maturation

A benefit of a mouse model is that it allows us to track the activation and differentiation of B cells in vivo. Thus, we crossed the *Pik3cd*^{E1020K} GOF mice to transgenic mice expressing a BCR recognizing hen egg lysozyme (HEL), hereafter referred to as SW_{HEL} mice (Brink et al., 2015). To determine the intrinsic effect of overactive PI3K on B cell responses, we transferred WT or *Pik3cd*^{E1020K} GOF SW_{HEL} cells to congenic WT recipients which were then immunized with SRBC conjugated to a lower affinity variant of HEL (HEL-2x) (Brink et al., 2015). When tracked over a 10-d period, expansion of the *Pik3cd*^{E1020K} GOF B cells was comparable to WT B cells (Fig. 8 A). Similarly we saw no difference in the percentages of SW_{HEL} B cells that became plasmablasts or GC cells (Fig. 8 B), suggesting PI3K activity does not control the decision between plasmablast and GC fates. In this SW_{HEL}/SRBC system a large proportion of responding B cells switch to IgG1 (Brink et al., 2015). Analysis of B cell subsets revealed that ∼50% fewer *Pik3cd*^{E1020K} GOF plasmablasts and GC B cells had switched to IgG1 compared with WT B cells (Fig. 8 C). Again, this was not due to an increase in switching to alternative isotypes, as ∼2-fold more *Pik3cd*^{E1020K} GOF B cells continued to express IgM (Fig. 8 C). To determine how this affected production of Ag-specific antibodies we measured serum levels of anti-HEL antibody of various isotypes 5 d after immunization. Mice that received *Pik3cd*^{E1020K} GOF SW_{HEL} B cells had a fivefold increase in the levels of anti-HEL IgM antibody (Fig. 8 D), consistent with the hyper-IgM phenotype often observed in *PIK3CD* GOF patients (Coulter et al., 2017). Despite the decreased percentage of switched $IgG1^+$ cells we saw no significant decrease in serum IgG1 in *Pik3cd*^{E1020K} GOF compared with WT mice (Fig. 8 D). We also measured levels of serum IgG2a, IgG2b, and IgG3. There were trends for increased IgG3 and decreased IgG2b, but no significant change in IgG2a (Fig. 8 D; not shown). Similar results were also seen 10 d after immunization (not shown).

An important function of the GC is affinity maturation of the Ab response. To determine whether *Pik3cd*^{E1020K} GOF disrupts this process within the GC, we sorted $IgG1^+$ SW_{HEL} B cells from mice 10 d after immunization and sequenced the BCR to identify somatic mutations. The average number of mutations per sequence was similar between WT and *Pik3cd* GOF $IgG1^+$ SW_{HEL} B cells (2.6 vs. 2.5, $n = 84$ or 91), indicating that PI3K GOF did not affect the overall rate of SHM. Affinity maturation in

Figure 5. ***PIK3CD* GOF transitional B cells have impaired molecular responses to IL-21. (A and B)** Transitional B cells from healthy donors and *PIK3CD* GOF patients were cultured with CD40L alone or together with IL-21 and gene expression profiles for each were obtained by microarray. **(A)** Heat map of log_2-transformed expression values for genes induced by IL-21 and involved in plasmablast generation. **(B)** Heat map of log_2-transformed expression values for key driver genes that distinguish CD40L/IL-21–treated transitional B cells from healthy donors and *PIK3CD* GOF patients identified by NMF. **(C and D)** qPCR analysis of human tonsil B cell subsets (N, naive; M, memory; GC, germinal center; PC, plasma cells) showing differential expression of genes identified in B that are down-regulated (C) or up-regulated (D) in human PCs relative to other B cell populations. Values represent the mean ± SEM of experiments using tonsils from 4 different donors. **(E and F)** Transitional B cells from healthy donors or *PIK3CD* GOF patients were cultured with CD40L alone or together with IL-21 for 5 d. **(E)** Proportions of $CD27^{hi}CD38^{hi}$ plasmablasts generated in these cultures were determined by flow cytometry. Contour plots are representative of data obtained from two to three independent experiments using transitional B cells isolated from different healthy donors or *PIK3CD* GOF patients. **(F)** Relative expression levels of the indicated genes were determined in transitional B cells by qPCR. Data are expressed as mean fold change (±SEM; $n = 3$) of gene expression in transitional B cells stimulated with CD40L/IL-21 relative to transitional B cells stimulated with CD40L alone. The dashed line represents a fold-change of 1.0, indicating no change in the presence versus the absence of IL-21 by CD40L-stimulated transitional B cells.

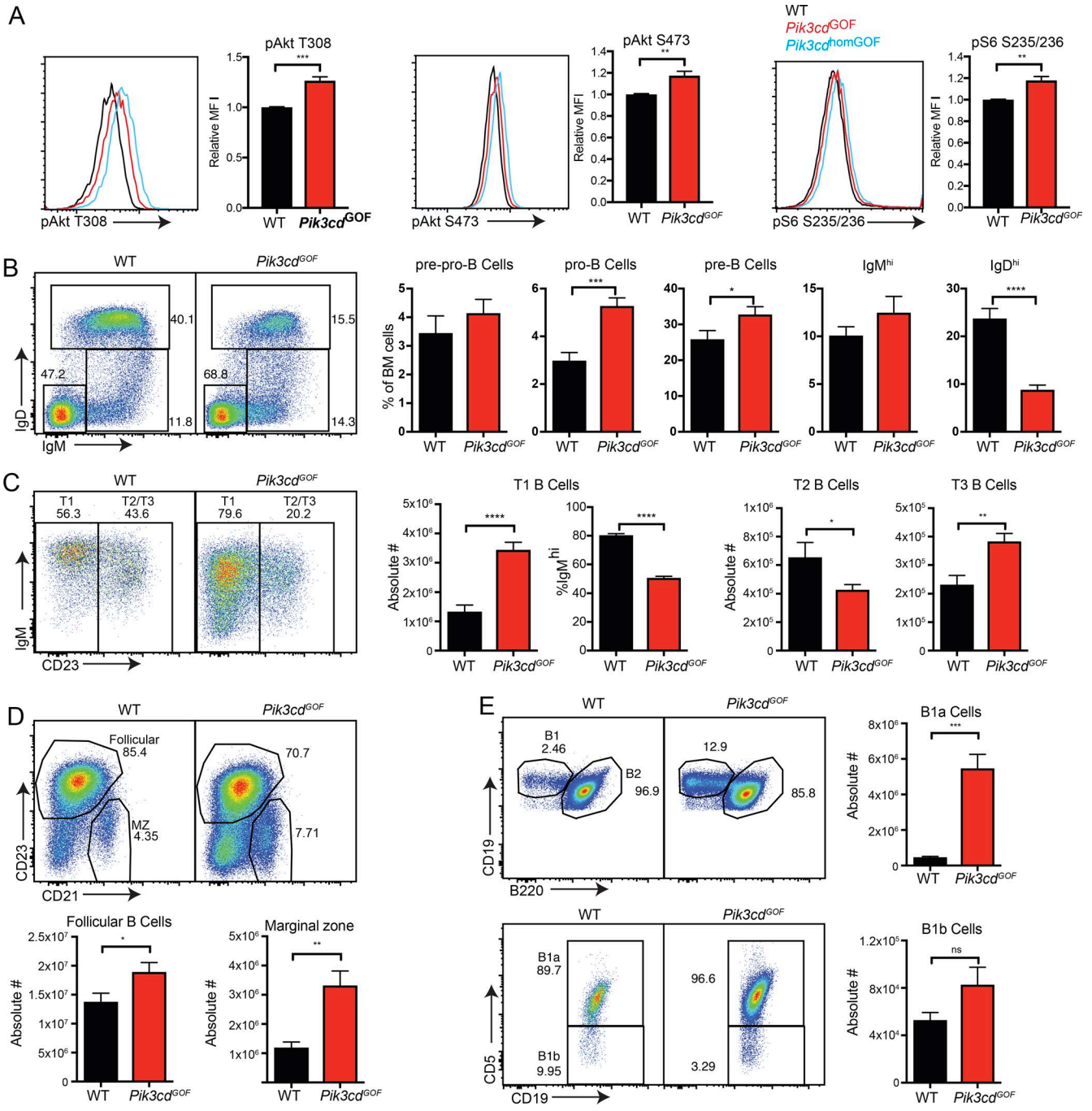

Figure 6. **Mice with overactive PI3K show aberrant B cell development. (A)** B cells were stained intracellularly for phosphorylated Akt (T308 and S473) and S6 (S235/236). Histograms show representative staining from WT (black), *Pik3cd*^{E1020K} heterozygous (*Pik3cd*^{GOF}, red), or *Pik3cd*^{E1020K} homozygous (*Pik3cd*^{homGOF} blue) mice and graphs give MFI relative to WT controls (mean ± SEM, *n* = 5). **(B–D)** BM and spleens from WT and *Pik3cd*^{E1020K} heterozygous GOF mice aged 8–12 wk were stained to identify different B cell populations. **(B)** B cell development in the BM. Flow cytometry plots showing representative staining of IgD versus IgM on B220$^+$ cells. Numbers are percent IgM$^-$IgD$^-$, IgM^{hi}, and IgD^{hi} cells. IgM$^-$IgD$^-$ cells were further gated on CD24 and CD43 to identify pre-pro–, pro- and pre-B cells. Graphs give mean ± SEM (*n* = 9–12). **(C)** Transitional cells in the spleen. Flow plots show IgM versus CD23 on B220$^+$CD93$^+$ cells. Graphs show absolute numbers of T1 and T2/T3 cells as well as the percentage of each population that is IgM^{hi} (mean ± SEM, *n* = 9–12). **(D)** Percentages of follicular (CD23$^+$CD21^{lo}) and MZ (CD21^{hi}CD23^{lo}) B cells were determined in the mature B cell population (CD93$^-$) of the spleen. Flow plots show representative staining of CD21 versus CD23. Graphs show absolute numbers of follicular and MZ cells (mean ± SEM, *n* = 10–13). **(E)** Percentages of B1a (CD19$^+$B220^{lo}CD5$^+$) or B1b (CD19$^+$B220^{lo}CD5$^-$) cells were determined. Flow plots show representative staining of B220 versus CD19 gated on CD19$^+$ cells (upper panel) and CD19 versus CD5 gated on CD19$^+$B220^{lo} cells (lower panel). Graphs show absolute numbers of B1a and B1b cells in the spleen (mean ± SEM, *n* = 6–8). Significant differences were determined by unpaired Student's *t* tests. *, P < 0.05; **, P < 0.01; ***, P < 0.001; ****, P < 0.0001.

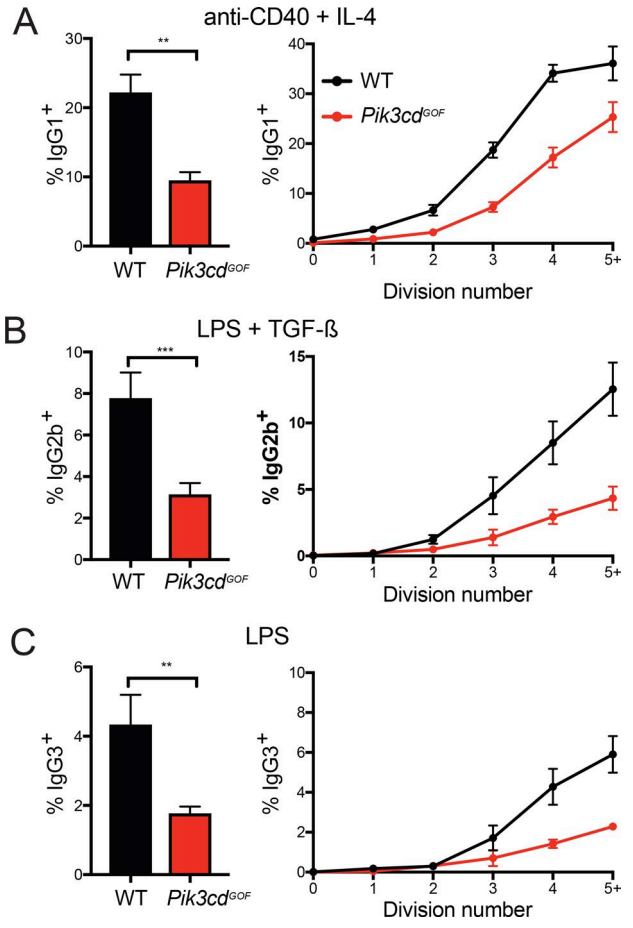

Figure 7. ***Pik3cd* GOF B cells show a division-related decrease in switching to multiple IgG isotypes. (A–C)** Follicular B cells ($B220^+CD93^-CD23^+CD21^{lo}$) were sorted from the spleens of WT or *Pik3cd*^{GOF} mice. Cells were labeled with CFSE and stimulated with anti-CD40 + IL-4 (A), LPS + TGF-β (B) or LPS alone (C) for 4 d after which they were stained for IgG1, IgG2b and IgG3 as shown. Left panels show total percentage of cells of each isotype. Right panels show the percentage of switched cells in each division as determined by CFSE. Plots show mean ± SEM, $n = 4–6$. Significant differences were determined by paired *t* tests. **, $P < 0.01$; ***, $P < 0.001$.

SW_{HEL} B cells responding to HEL-2x is associated with a Y53D mutation, which greatly increases affinity of the receptor for the mutant HEL (Brink et al., 2015). By day 10, >50% of WT cells acquired the Y53D mutation (Fig. 8 F). A similar percentage of *Pik3cd*^{E1020K} GOF B cells were also found to have the Y53D mutation, indicating that increased PI3K activity did not affect affinity maturation.

Thus despite the many reported roles of PI3K in controlling B cell function, as revealed by germline modification of genes encoding p110δ, p85, or PTEN (Fruman et al., 1999; Suzuki et al., 1999, 2003; Clayton et al., 2002; Jou et al., 2002; Okkenhaug et al., 2002; Anzelon et al., 2003; Omori et al., 2006; Dengler et al., 2008; Srinivasan et al., 2009), we found that during an in vivo TD response the primary defect was in switching to IgG. In contrast, other functions such as expansion, GC formation and affinity maturation remained intact.

Inhibition of hyperactive PI3K signaling partially overcomes defects in B cell differentiation

Inhibitors of p110δ have been developed and used to treat several human B cell malignancies (Hewett et al., 2016; Fruman et al., 2017). Leniolisib is a recently developed specific inhibitor of p110δ (Hoegenauer et al., 2017) and has shown safety and clinical efficacy in treating six patients with *PIK3CD* GOF mutations, including partial corrections of B cell subsets and serum IgM levels (Rao et al., 2017). However it is unknown whether the favorable clinical outcome on humoral immunity results from a direct effect on B cells or is secondary to effects on other immune cell types, such as $CD4^+$ T cells (Rolf et al., 2010). To explore this in more detail, we determined whether leniolisib could improve the function of human and murine B cells with hyperactive PI3K signaling. We examined Ig secretion and class switching by B cells following in vitro stimulation, as defects in these processes were the most robust phenotype observed (Figs. 4 and 7). The concentrations of leniolisib tested were optimized to have a minimal effect on B cell proliferation and survival (not shown). When transitional B cells from healthy donors were cultured with CD40L/IL-21, leniolisib resulted in a concentration-dependent decrease in secretion of IgM and IgG, but had no effect on IgA (Fig. 9, A–C). In contrast, leniolisib had no effect on IgM secretion by *PIK3CD* GOF transitional B cells, but resulted in significant increases in secretion of the class switched isotypes IgG and IgA (Fig. 9, A–C).

To more directly assess CSR, we cultured murine B cells with anti-CD40/IL-4 and various doses of leniolisib. Leniolisib increased the percentage of $IgG1^+$ cells generated from both WT and *Pik3cd*^{E1020K} GOF B cells (Fig. 9 D). Importantly, the class switch defect in *Pik3cd*^{E1020K} GOF murine B cells was completely restored by inhibiting p110δ (Fig. 9 D). Division analysis revealed that this was due to a dramatic increase in switching in the earlier divisions such that, at the higher dose of leniolisib, >20% of both WT and *Pik3cd*^{E1020K} GOF B cells that had undergone one division had switched to IgG1 compared with <2% in control cultures (Fig. 9 E). Interestingly, while similar switching was observed between WT and GOF cells at the higher dose of leniolisib, at the lower dose there remained a difference between WT and *Pik3cd*^{E1020K} GOF B cells, indicating a dose-dependent relationship between PI3K activation and switching.

To gain insight into the molecular mechanism for reduced CSR due to PI3K p110δ GOF, we performed qPCR on WT and *Pik3cd*^{E1020K} GOF B cells to establish expression levels of genes involved in regulating B cell differentiation. *Bcl6* and *Prdm1* were expressed at normal levels in activated *Pik3cd*^{E1020K} GOF murine B cells (not shown). However, induction of *Aicda* was significantly impaired in *Pik3cd*^{E1020K} GOF murine B cells following stimulation with anti-CD40L/IL-4 (Fig. 9 F). Strikingly, treatment of *Pik3cd*^{E1020K} GOF B cells with leniolisib restored *Aicda* expression to levels observed in WT B cells (Fig. 9 F). Notably, *Aicda* was also increased in leniolisib-treated WT B cells, consistent with increased class switching to IgG1 by these B cells in the presence of increasing doses of this p110δ inhibitor (Fig. 9 D, E). Indeed, plotting *Aicda* expression versus $IgG1^+$ B

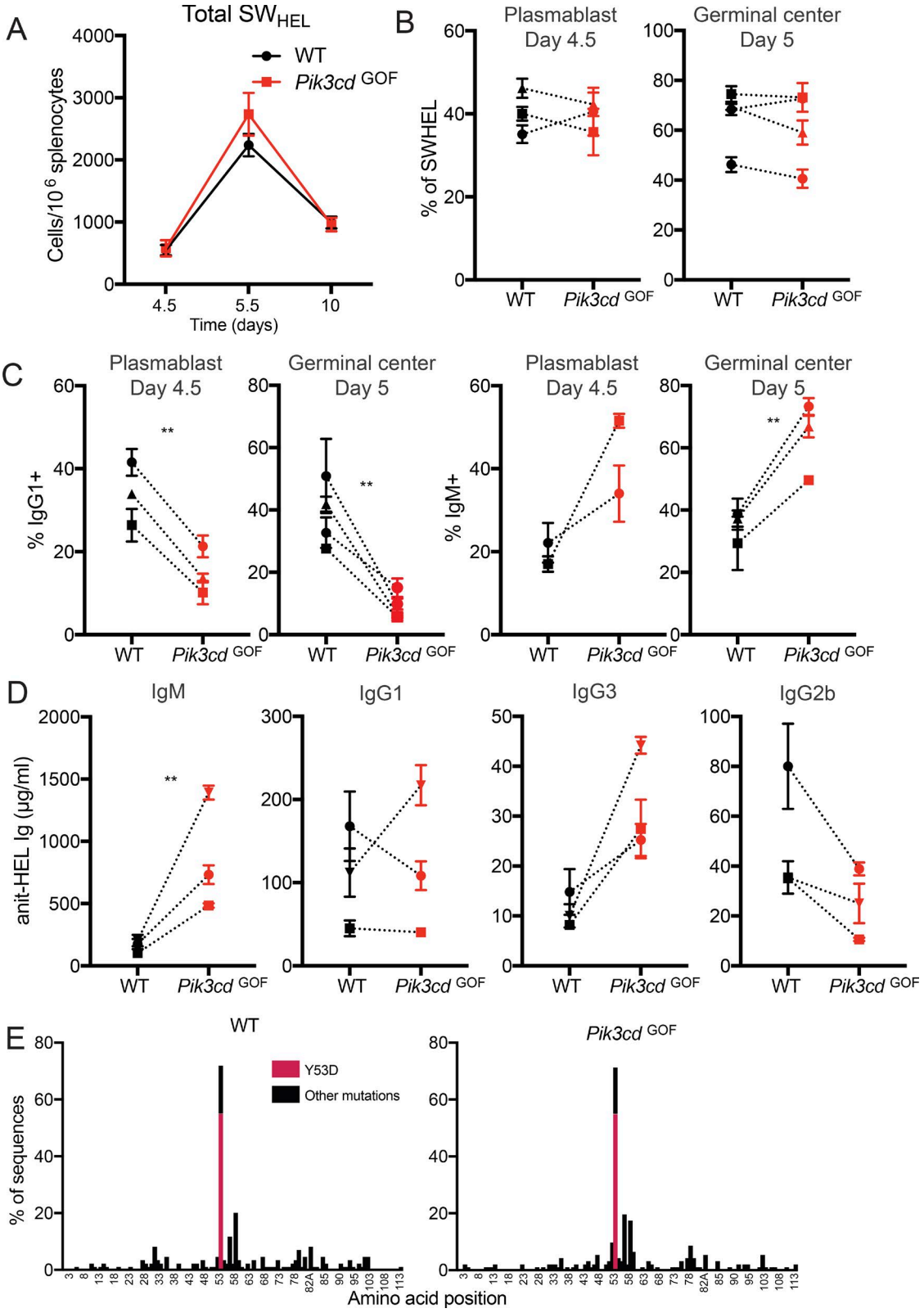

Figure 8. ***Pik3cd* GOF B cells show defective switching but normal expansion and affinity maturation in vivo.** WT or *Pik3cd*^{GOF} SWHEL cells were transferred to WT congenic hosts, which were then immunized with HEL-2x-SRBC. **(A)** The expansion of SW_{HEL} cells was tracked over time (mean ± SEM, n = 3–4 mice per group, representative experiment shown). **(B)** Percentage of cells with a plasmablast or GC phenotype was determined. **(C)** Percentage of cells that switched to IgG1 or were unswitched (IgM^+) was determined in the plasmablast and GC populations. **(D)** Levels of HEL-specific serum Ig of various classes at day 5.5 were determined by ELISA. (B–D, each linked point shows mean ± SEM [n = 3–5] of single experiment). **(E)** Donor GC $IgG1^+$ cells were sorted on day 10 and sequenced to identify mutations. Significant differences were determined by paired t tests. **, $P < 0.01$.

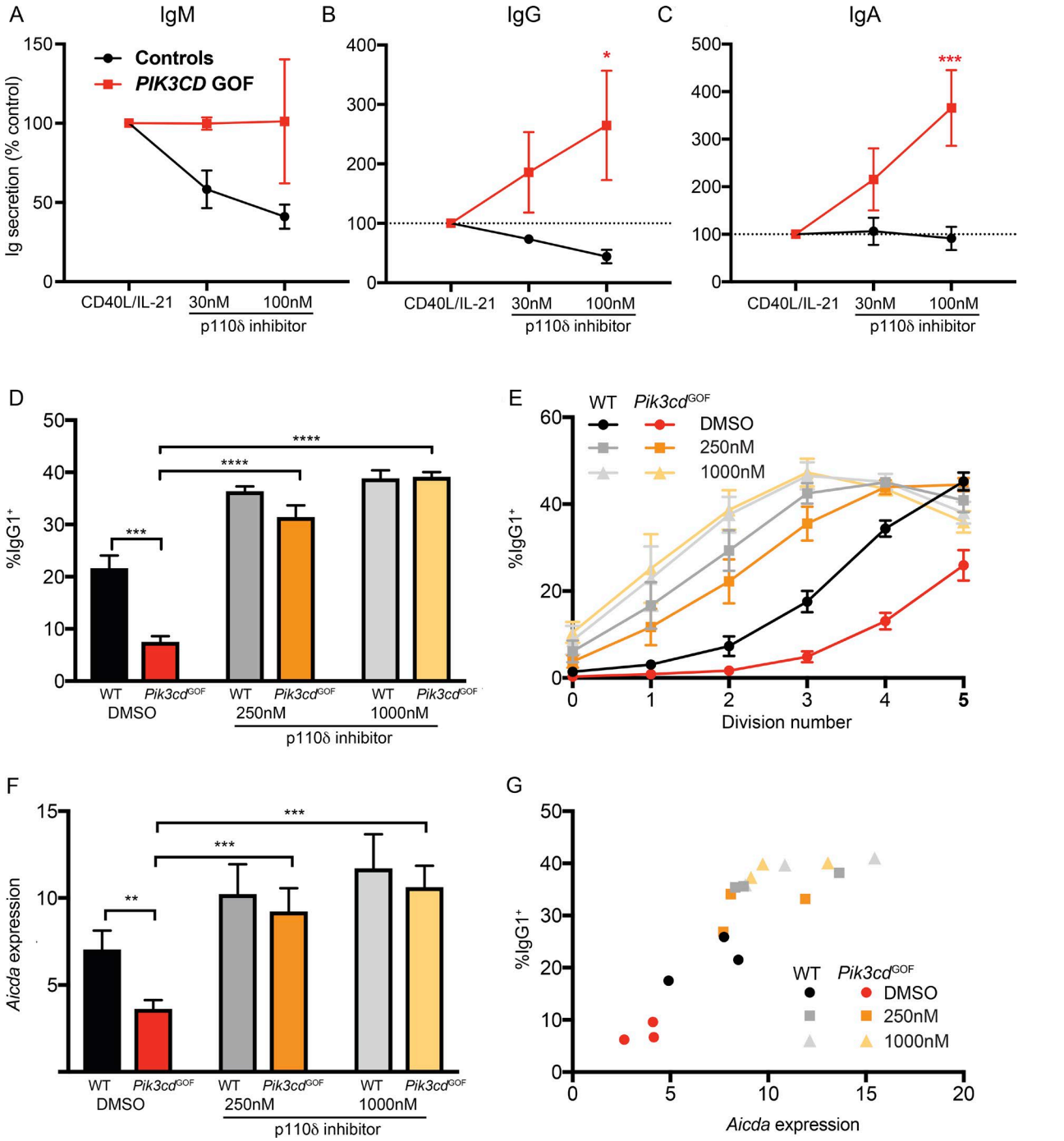

Figure 9. **A p110δ inhibitor partially alleviates the defects in B cell differentiation due to hyperactive PI3K signaling. (A–C)** Sort-purified transitional B cells from healthy donors or *PIK3CD* GOF patients (n = 5) were cultured for 5 d with CD40L plus IL-21 in the absence or presence of the PI3K p110δ inhibitor leniolisib. Secretion of (A) IgM, (B) IgG, and (C) IgA was then determined. Data are expressed as mean percentage of Ig secreted (± SEM) by B cells stimulated with CD40L/IL-21. **(D–G)** Follicular B cells ($B220^+CD93^-CD23^+CD21^{lo}$) were sorted from the spleens of WT or $Pik3cd^{GOF}$ mice. Cells were labeled with CFSE and stimulated with anti-CD40 + IL-4 in the absence or presence of leniolisib for 4 d. **(D and E)** Cells were stained for expression of IgG1 and the total percentage of IgG1+ B cells detected (D) and the % of IgG1+ B cells in each division as determined by CFSE dilution (E) were determined. **(F)** Expression of *Aicda* in WT or $Pik3cd^{GOF}$ B cells cultured with anti-CD40 + IL-4 was determined by qPCR. Plots show mean ± SEM, n = 3. **(G)** Plot of *Aicda* expression versus percentage IgG1+ cells generated following culture of WT or $Pik3cd^{GOF}$ B cells with anti-CD40 + IL-4 in the absence or presence of leniolisib. Significant differences were determined by two-way ANOVA. **, P < 0.01; ***, P < 0.001; ****, P < 0.0001.

cells for WT and $Pik3cd^{E1020K}$ GOF B cells in the absence and presence of leniolisib revealed a very strong positive correlation (Fig. 9 G). Together, these data reveal that activating mutations in PI3K p110δ impede Ig CSR by reducing AID expression in B cells. Furthermore, pharmacological targeting of the PI3K pathway with leniolisib corrects defects in B cell differentiation by relieving the inhibitory effect of hyperactive PI3K signaling on AID expression.

Discussion

Signaling via PI3K plays a fundamental role in immune function, immune regulation, and humoral immunity. This is evidenced from phenotypes arising in mice with germline deletion or inactivation of the p110δ or p85 subunits of PI3K (Fruman et al., 1999; Suzuki et al., 1999; Clayton et al., 2002; Jou et al., 2002; Okkenhaug et al., 2002; Srinivasan et al., 2009), or of PTEN (Anzelon et al., 2003; Suzuki et al., 2003; Sander et al., 2015) which antagonizes PI3K signaling. More strikingly, homozygous mutations in *PIK3R1* prevented B cell development in humans (Conley et al., 2012; Tang et al., 2018), while heterozygous germline mutations in *PIK3CD*, *PIK3R1*, or *PTEN* result in immune dysregulation evidenced by immunodeficiency, autoimmunity, and B cell malignancy (Jou et al., 2006; Angulo et al., 2013; Crank et al., 2014; Deau et al., 2014; Kracker et al., 2014; Lucas et al., 2014a,b; Hartman et al., 2015; Driessen et al., 2016; Elgizouli et al., 2016; Elkaim et al., 2016; Tsujita et al., 2016; Coulter et al., 2017). These observations from mice and humans underscore the critical requirement for regulated PI3K signaling for immune homeostasis and function. However, mechanisms underlying disease pathogenesis in humans remain incompletely determined.

By analyzing a large cohort of patients (n = 39) with activating mutations in *PIK3CD* and developing a novel mouse model of *Pik3cd*^{E1020K} GOF by CRISPR/Cas9-mediated genome editing, we have now revealed key functions for PI3K in B cell development and differentiation. B cell development in human BM was perturbed at the pre-BII and immature stages, with an aberrant accumulation of these cells and corresponding reductions in recirculating mature B cells. This extends a previous study that examined B cell development according to proportions of stage I, stage II, and stage III hematogones within all CD10$^+$ B cell precursors (Dulau Florea et al., 2017). Our finding that BM transplant corrected B cell development in *PIK3CD* GOF revealed that hematopoietic cell intrinsic defects were responsible for aberrant B cell development. Defective B cell development was also clear from our analysis of peripheral blood, as proportions of CD21^{lo} early transitional B cells (Suryani et al., 2010) were greatly increased in the patients, and these cells exhibited phenotypic and molecular features consistent with being less mature than CD21^{lo} transitional cells in healthy donors. This defect in B cell development was also observed in *Pik3cd*^{E1020K} GOF mice where increases in immature B cells were observed not only in the BM, but also in peripheral lymphoid organs and the circulation. *Pik3cd*^{E1020K} GOF mice also had increased numbers of B1 and MZ B cells, akin to B cell specific PTEN-deficient mice (Anzelon et al., 2003; Suzuki et al., 2003). Thus, mutations that result in PI3K p110δ GOF strongly compromise successful B cell development in the BM and periphery leading to a skewed B cell compartment.

PI3K p110δ GOF also resulted in several functional B cell defects. Memory B cells were reduced in *PIK3CD* GOF patients. Among the contracted population of memory B cells, the proportions that had undergone Ig isotype switching were significantly reduced. By studying our *Pik3cd*^{E1020K} GOF mouse model we confirmed that this in vivo defect in switching was B cell intrinsic and affected all IgG subclasses. Activated PI3K p110δ GOF B cells from humans and mice exhibited defective class switching and secretion of IgG and IgA. Murine PI3K p110δ GOF B cells expressed lower levels of *Aicda* mRNA than WT B cells. Importantly, the p110δ inhibitor leniolisib improved secretion of IgG and IgA by *PIK3CD* GOF human B cells, and completely restored not only CSR but also *Aicda* expression in *Pik3cd*^{E1020K} GOF murine B cells. Indeed, manipulating PI3K function either by introduction of the GOF allele or inhibition with leniolisib revealed a strong correlation between PI3K activity, AID expression, and IgG class switching. Thus, the molecular mechanism underlying impaired CSR due to PI3K GOF most likely results from reduced expression of AID. This conclusion concurs with previous studies suggesting PI3K regulates CSR in murine B cells by repressing AID (Omori et al., 2006; Dengler et al., 2008; Compagno et al., 2017). Further analysis of the microarray data using the REACTOME database revealed significantly greater expression of components of pathways involved in DNA damage responses in activated transitional B cells from healthy donors than from *PIK3CD* GOF patients (Table S1). The DNA damage response is required to maintain genomic stability and is induced in response to the AID-mediated DNA breaks that are necessary for CSR (Daniel and Nussenzweig, 2013). This is further evidence of reduced AID function due to hyperactive PI3K p110δ, which underlies impaired CSR in these B cells. Alternatively, decreased expression of molecules involved in the DNA damage response and AID-mediated mismatch repair, such as *EXO1* (Table S1; Eccleston et al., 2011) may themselves compromise CSR. It is also possible that B cell extrinsic defects arising from PI3K p110δ GOF, such as compromised function of CD4$^+$ T cells, especially Tfh cells (Rolf et al., 2010), compound these B cell intrinsic defects in effector function. This is currently being investigated.

In contrast to decreased CSR, SHM (which is also dependent on AID; Durandy et al., 2007) was intact in murine PI3K p110δ B cells, suggesting that the decrease in AID expression detected was insufficient to ablate the function of AID in SHM. This is consistent with impaired class switching (Fig. 1), but intact SHM (Angulo et al., 2013), in memory B cells from *PIK3CD* GOF individuals, and also the discovery of some patients with biallelic mutations in the C-terminal domain of *AICDA* whose B cells are unable to undergo CSR but exhibit normal levels of SHM (Durandy et al., 2007).

Although *PIK3CD* GOF B cells exhibited hallmarks of Ig-secreting cell differentiation in vitro (IgM secretion and BLIMP-1 expression), the magnitude and quality of this process was compromised, particularly in transitional B cells. These differences in Ig secretion by transitional B cells from controls and *PIK3CD* GOF patients may reflect differences in the composition of the transitional B cell populations being compared. However, this is unlikely because we previously showed that CD21^{lo} and CD21^{hi} transitional B cell subsets from healthy donors produce comparable amounts of IgM, IgG, and IgA in vitro (Suryani et al., 2010). Rather, this defect arose from the inability of *PIK3CD* GOF transitional B cells to acquire or maintain a plasmablast phenotype and gene signature following in vitro activation. Indeed, *PIK3CD* GOF transitional B cells were impaired in generating CD38^{hi} CD27^{hi} plasmablasts in vitro. Here, the detected IgM secreted by these cells is likely produced by preplasmablasts that have not yet acquired the phenotype and transcriptional profile of plasmablasts (Avery et al., 2005; Jourdan et al., 2011). The finding

that *PAX5* was down-regulated less in activated PI3K p110δ GOF human transitional B cells compared with normal B cells may contribute to the altered gene expression profile and impaired Ig secretion by these cells, since loss of PAX5 function is a prerequisite for the differentiation and commitment of B cells to the PC fate (Kallies et al., 2007). Thus, it would be expected that the increased numbers of immature transitional cells and their decreased function, coupled with impaired survival and trafficking due to poor expression of Bcl2 and homeostatic chemokine receptors, would combine to greatly impact the level of functional antibody produced in PI3K GOF patients. Interestingly, our microarray analyses revealed increased *IL10* expression by *PIK3CD* GOF transitional B cells compared with controls. Human transitional B cells have been proposed as being a rich source of IL-10 (Blair et al., 2010). But this is not unique to transitional cells, because naive, memory and GC B cells can all secrete IL-10 following in vitro stimulation (Burdin et al., 1996; Good et al., 2006). Interestingly, IL-10 is a growth and differentiation factor for human B cells, and endogenous IL-10 contributes to B cell differentiation induced by CD40L/BCR engagement (Moens and Tangye, 2014). However, despite the ability of IL-10 to promote B cell differentiation, the potential elevated expression of *IL10* by *PIK3CD* GOF transitional B cells was insufficient to rescue the defect in CD40L/IL-21–mediated differentiation of these cells in vitro.

The PI3K/AKT/mTOR pathway is activated in 40–50% of cases of diffuse large B cell lymphoma (Xu et al., 2013). Furthermore, PI3K p110δ inhibitors have been used to treat human B cell malignancies (Hewett et al., 2016; Fruman et al., 2017). Thus, it is possible that *PIK3CD* GOF mutations intrinsically contribute to B cell lymphomagenesis, which occurs in ∼20% of *PIK3CD* GOF patients (Coulter et al., 2017). However, PI3K inhibitors increase AID expression and activity in murine and human B cells, causing increased genomic instability in vitro and lymphomagenesis in vivo (Compagno et al., 2017). Our finding of reduced levels of AID in PI3K p110δ GOF B cells could infer that *PIK3CD* activating mutations are not directly oncogenic. Rather, B cell lymphoma may result from impaired effector function of *PIK3CD* GOF NK and $CD8^+$ T cells (Edwards et al., 2018; Ruiz-García et al., 2018). The etiology and mechanisms underlying lymphoma development in *PIK3CD* GOF patients is an area requiring further investigation. Determining whether PI3K p110δ inhibitors (Rao et al., 2017) influence the incidence of B cell lymphoma may provide valuable insight into these outstanding questions.

Collectively, these data provide significant insight into the pathological mechanisms underlying hyper-IgM, hypogammaglobulinemia, and impaired long-lived humoral immune responses in *PIK3CD* GOF patients (Jou et al., 2006; Angulo et al., 2013; Lucas et al., 2014a; Elgizouli et al., 2016; Coulter et al., 2017). Our data also identify putative regulatory networks in B cells that are controlled by PI3K signaling and may play a role in PC differentiation. Importantly, the impairment in secretion of switched Ig isotypes by human *PIK3CD* GOF transitional B cells, and in class switching and *Aicda* expression by $Pik3cd^{E1020K}$ GOF murine B cells, could be greatly improved by the PI3K p110δ inhibitor leniolisib. Based on these results leniolisib may improve the ability of patients to generate effective switched Ab responses, eventually resulting in a requirement for Ab replacement therapy, which is currently used in >80% of patients (Coulter et al., 2017). The efficacy of leniolisib in treating *PIK3CD* GOF patients (Rao et al., 2017), and our demonstration that it improves B cell function in vitro, suggests p110δ inhibitors could be suitable therapeutics for other immune dysregulatory conditions due to defects in PI3K signaling. These include individuals not only with *PIK3CD* GOF mutations, but also those with inactivating mutations in *PIK3R1* (Deau et al., 2014; Lucas et al., 2014b; Elkaim et al., 2016) or *PTEN* (Driessen et al., 2016; Tsujita et al., 2016), or even patients with clinical features overlapping these conditions but with hitherto unknown genetic diagnoses (Deenick et al., 2018). However, such treatment will need to be monitored carefully to mitigate the potential risk of accelerating or exacerbating lymphoma development in these patients.

Overall, our detailed analysis has provided insight into the pathophysiology of disease due to *PIK3CD* GOF mutations. Furthermore, our observations that the $Pik3cd^{E1020K}$ GOF mutation in murine B cells mirrored the effects of *PIK3CD* GOF mutations in humans underscores the utility of this mouse model to investigate the consequences of hyperactive PI3K signaling and to dissect mechanisms of disease pathogenesis in humans with corresponding mutations. Thus, these mice represent a valuable preclinical model to screen new or alternative pharmacological or biological inhibitors of the PI3K pathway as novel therapeutics for humans with *PIK3CD* GOF mutations.

Materials and methods

Human blood and bone marrow samples

Buffy coats from healthy donors were purchased from the Australian Red Cross Blood Service. Pediatric blood samples were collected from individuals either attending clinic for nonimmunological conditions, or for genetic testing due to a family history of disease, but were found to be mutation negative. BM was obtained from individuals undergoing lymphoma staging, and was found to be uninvolved. Peripheral blood and BM samples were also collected from patients with GOF mutations in *PIK3CD*. Human tonsils were obtained from healthy donors undergoing routine tonsillectomy (Mater Hospital, North Sydney). Approval for this study was obtained from the human research ethics committees of St. Vincent's Hospital (Sydney, Australia), Sydney South West Area Health Service (Sydney, Australia), Royal Children's Hospital Melbourne (Melbourne, Australia), and the National Institute of Allergy and Infectious Diseases Intramural Institutional Review Board (Bethesda, MD); informed consent was obtained from all participants for human experiments described in this study.

Human antibodies

The following mAbs were used: FITC-anti CD20, PE-Cy7-anti-CD27, APC-anti-CD10, PE-anti-CD5, APC-anti-CD38, BV421-anti-CD21, biotin anti-CD44, BV711-anti-CD19, FITC anti-CCR7 (CD197), PE anti-CXCR4 (CD184), biotin anti-CXCR5 (CD185), PE-anti-IgM, BV605-anti-IgG, biotin-anti-IgA, PE-anti-Bcl-2, PE-anti-Blimp-1, Streptavidin-BV605, and Streptavidin-PerCP-Cy5.5 (all from Becton Dickinson); PE-anti-CD23 and FITC-anti-CD38 (eBioscience); and biotin-anti-IgD (Southern Biotech).

Human lymphocyte phenotyping

PBMCs were incubated with mAbs against CD20, CD27, and CD10 with mAb specific for CD5, CD38, CD21, CD23, CD44, CD19, CCR7, CXCR4, CXCR5, and Bcl-2. The proportions of $CD20^+CD27^-CD10^+$ (transitional), $CD20^+CD27^-CD10^-$ (naive), and $CD20^+CD27^+CD10^-$ (memory) B cells, as well as the expression of these molecules on these subsets, was determined by flow cytometry (LSRII SORP; Becton Dickinson) and analyzed using FlowJo software (Tree Star; Cuss et al., 2006; Suryani et al., 2010). BM aspirates were incubated with mAbs against CD34, CD19, CD20, CD10, IgM, and CD27. Populations of pro-B ($CD19^+CD34^+CD10^+CD20^-IgM^-$), preBI ($CD19^+CD34^-CD10^+CD20^-IgM^-$), preBII ($CD19^+CD34^-CD10^+CD20^{dim}IgM^-$), immature ($CD19^+CD34^-CD10^+CD20^+IgM^+$), and recirculating mature ($CD19^+CD34^-CD10^-CD20^+$) B cells were quantified (Uckun, 1990; van Zelm et al., 2005).

Isolation and in vitro activation of human B cell subsets

PBMCs were labeled with mAbs against CD20, CD27, and CD10 and transitional ($CD20^+CD10^+CD27^-$) or naive ($CD20^+CD10^-CD27^-$) B cells were then sorted using a FACSAria III (Becton Dickinson; Cuss et al., 2006; Suryani et al., 2010). Purity of the recovered populations was >98%. Transitional and naive B cells were then cultured in 96-well U-bottom plates (Falcon; 20–40 × 10^3/200 µl well) for 4–5 d to determine proliferation and gene expression by qPCR and microarray analysis, or 5 × 10^3/200 µl well for 5–7 d to determine Ig secretion. B cells were stimulated with 200 ng/ml CD40L cross-linked to 50 ng/ml HA Peptide mAb (R&D Systems) alone or together with 100 U/ml IL-4, 100 U/ml IL-10 (provided by R. de Waal Malefyt, DNAX Research Institute, Palo Alto, CA), 50 ng/ml IL-21 (PeproTech), 2.5 µg/ml $F(ab')_2$ fragment of goat anti-IgA/IgG/IgM (H+L; Jackson ImmunoResearch), 1 µg/ml CpG 2006 (Sigma-Aldrich), and varying doses of the PI3K p110δ specific inhibitor leniolisib (Hoegenauer et al., 2017; Rao et al., 2017; Novartis Pharma), and equivalent doses of DMSO.

Analysis of human B cell Differentiation in vitro.

B cell viability was determined using the Zombie Aqua Viability dye (BioLegend) and proliferation determined by CFSE (eBioscience) dilution after 4–5 d of in vitro culture (Avery et al., 2010). Differentiation of B cells to plasmablasts was assessed by determining the frequency of transitional or naive B cells acquiring a $CD38^{hi}$ $CD27^{hi}$ phenotype during in vitro culture (Avery et al., 2005, 2010). To determine expression of intracellular Ig and Blimp-1, cells were initially labeled with mAbs to CD27 and CD38, then fixed and permeabilized (Foxp3/Transcription Factor Staining Buffer; eBioscience). Permeabilized cells were then incubated with a cocktail of mAbs to IgG, IgM, IgA, and Blimp-1 and expression of these proteins in plasmablasts was determined by flow cytometry (LSRII SORP; Becton Dickinson) and analyzed using FlowJo software (Tree Star).

qRT-PCR

Total RNA was isolated from unstimulated FACS-sorted transitional and naive B cells from normal donors or *PIK3CD* GOF patients using an RNeasy Mini Kit (QIAGEN). PCR primers (Integrated DNA Technologies) were designed using the Roche UPL primer design program. Primer sequences and Roche UPL probes are as follows: *GAPDH*, UPL probe 60, forward 5′-CTCTGCTCC TCCTGTTCGAC-3′; reverse 5′-ACGACCAAATCCGTTGACTC-3′; *RPL13A* (*Ribosomal Protein L13a*), UPL probe 28, forward 5′-CAA GCGGATGAACACCAAC-3′, reverse 5′-TGTGGGGCAGCATACCTC-3′, *LEF1* (*Lymphoid enhancing binding factor-1*), UPL probe 17, forward 5′-CAGATGTCAACTCCAAACAAGG-3′, reverse 5′-GGA GACAAGGGATAAAAAGTAGGG-3′; *DTX1* (*Deltex-1*), UPL probe 57, forward 5′-GGGGCAGAACAACCTCAAC-3′, reverse 5′-CAAGTT CTTCACCGGGAGTG-3′ (Suryani et al., 2010).

To assess gene expression in activated B cells, total RNA was isolated from B cells cultured with CD40L ± IL-21 for 4–5 d. Primer sequences and Roche UPL probes were: *PRDM1 (PR Domain Zinc Finger Protein 1*), UPL probe 67, forward 5′- ACGTGTGGGTACGAC CTTG-3′, reverse 5′-CTGCCAATCCCTGAAACCT-3′; *AICDA (Activation-Induced Cytidine Deaminase*), UPL probe 69, forward 5′-GAC TTTGGTTATCTTCGCAATAAGA-3′, reverse 5′-AGGTCCCAGTCC GAGATGTA-3′; *MS4A7*, UPL probe 31, forward 5′-GGATCCAGTAAT GCCAAAACA-3′, reverse 5′-CCTACCCCTCCCACTTCAAT-3′; *PTPRJ*, UPL probe 6, forward 5′-TTGACTAATTCCAACAAGCTTCAG-3′, reverse 5′-CAGCAAGCTGACTCCAACTG-3′; *GPR15*, UPL probe 77, forward 5′-GTCCAATTTAGAGCCCAGTATGA-3′, reverse 5′-GGGCCT TTCCTCTCTCAAAA-3′; *SIGLEC6*, UPL probe 8, forward 5′-CTC CCAGGACACCACCAG-3′, reverse 5′-GCTCCCTGCAAATCTCTCTG-3′; ZNF215, UPL probe 82, forward 5′-TTAAGTGGCAAATGATGA ACAAA-3′, reverse 5′-GCTCCCTTCACTGTCCAAGA-3′; *MYO1D*, UPL probe 2, forward 5′-TTCTGAACCTCCTTGGAGTAGC-3′, reverse 5′-AGAAAAGTCTCGAGTGATTGTGC-3′; *KMO*, UPL probe 90, forward 5′-AAAAAGAGTCCTTTGTTTATCACCTT-3′, reverse 5′-CCATCGACCTTTATCCCTCTC-3′; *SLAMF7*, UPL probe 67, forward 5′-TTTAGGCTTTGACAGGTGCTC-3′, reverse 5′-TCTACTATG TGGGGATATACAGCTCA-3′; *BEX5*, UPL probe 44, forward 5′-GCA CAAACGCACTTAAAGACC-3′, reverse 5′-CTCGCTGTTGCCCTG AAG-3′; *RAP1GAP2*, UPL probe 38, forward 5′-CGCTCATGTACC GTCTTCAG-3′, reverse 5′-TTGATCCTGTCCGTCAAGTG-3′; *CD27*, UPL probe 30, forward 5′-TGGCCTCCAGCATCTCAC-3′, reverse 5′-CCTACCCCTCCCACTTCAAT-3′; *MS4A7*, UPL probe 31, forward 5′-GGATCCAGTAATGCCAAAACA-3′, reverse 5′-TCCAAACCCTTC GCTGAC-3′. All amplification reactions were performed using the Roche LightCycler 480 Probe Master Mix and System (Roche Diagnostics) with the following conditions: denaturation at 95°C for 10 min; amplification, 45 cycles at 95°C for 10 s, 65°C for 30 s, and 72°C for 5 s, and cooling at 40°C for 30 s. All reactions were standardized to the housekeeping gene *RPL13A* (Avery et al., 2010).

Microarray analysis

RNA was extracted from transitional and naive B cells, cultured for 4 d with CD40L alone or together with IL-21, and transcribed into cDNA. Raw gene expression data were obtained using the human Clariom S Assay microarray platform. All preprocessing and analyses were performed using Bioconductor packages implemented in the R statistical computing environment, version 3.4.1. The datasets were merged and batch corrected using ComBat of the sva package. Differential gene expression analysis was assessed using limma. Heat maps were generated using the pheatmap package. Unsupervised dimension reduction and metagene extraction was performed with the *NMF* package, as

previously described (Brunet et al., 2004; Kim and Park, 2007). Gene set enrichment analysis was performed using the gene set enrichment analysis module of GenePattern, hosted by the Broad Institute. Pathway analysis was performed using the Reactome FI plugin in Cytoscape 3.5.1. The microarray data are available on GEO under deposit number GSE116999.

RNA-seq analysis

Naive, memory, GC, and plasma cells were sorted from tonsils from healthy donors and subjected to RNA sequencing. RNA-seq reads were aligned to the GRCh37/hg19 build of the human genome using the Subread aligner (Liao et al., 2013). Genewise counts were obtained using featureCounts (Liao et al., 2014). Reads overlapping exons in annotation build 37.2 of NCBI RefSeq database were included. Genes were excluded from downstream analysis if they failed to achieve a CPM (counts per million mapped reads) value of 1 or greater in at least three libraries. Counts were converted to log2-CPM, quantile normalized and precision weighted with the voom function of the limma package (Law et al., 2014; Ritchie et al., 2015). A linear model was fitted to each gene, and empirical Bayes moderated t-statistics were used to assess differences in expression (Smyth, 2004).

Human Ig ELISAs

Secretion of IgM, IgG and IgA by in vitro cultured human transitional and naive B cells was determined using Ig heavy-chain specific ELISAs, as described previously (Avery et al., 2005, 2010).

Mice

Pik3cd^{E1020K} GOF mice were produced by the Mouse Engineering Garvan/ABR (MEGA) Facility using CRISPR/Cas9 gene targeting in C57BL/6J mouse embryos following established molecular and animal husbandry techniques (Yang et al., 2014). The single guide RNA (sgRNA) was based on a target site in the final exon of *Pik3cd* (GAG CTTCGTTGAACTTCACC*CGG*; protospacer-associated motif = PAM italicized and underlined) and was microinjected into the nucleus and cytoplasm of C57BL/6J zygotes together with polyadenylated *Streptococcus pyogenes* Cas9 mRNA and a 66 base single-stranded, anti-sense, deoxy-oligonucleotide homologous recombination substrate carrying the E1020K (GAA>AAA) mutation and a PAM-inactivating silent mutation in the F1014 codon (TTC>TTT; underlined nucleotides indicate those targeted by CRISPR and the subsequent change). A male founder mouse heterozygous for both substitutions was obtained and backcrossed with C57BL/6J female mice to establish the *Pik3cd*^{E1020K} GOF line. For some experiments these *Pik3cd*^{E1020K} GOF mice were then crossed with SW$_{HEL}$ mice (Brink et al., 2008, 2015) to generate SW$_{HEL}$.*Pik3cd*^{E1020K} GOF mice. Donor cells were adoptively transferred into C57Bl/6 (CD45.1 congenic) mice purchased from Australian BioResources. All experiments were approved by the Garvan Institute–St. Vincent's Animal Ethics Committee. Mice were bred and housed in SPF conditions at Australian BioResources (Moss Vale) and the Garvan Institute Biological Testing Facility.

In vitro culture of murine B cells

Spleens of *Pik3cd*^{E1020K} GOF or WT mice were harvested and prepared into single-cell suspensions. B cells were isolated using Miltenyi Biotec B cell isolation Kit and separated using Automacs Pro separator. Recovered B cells were then labeled with mAb against B220, CD23, CD21/35, and CD93 and follicular B (FOB) cells (B220^{+}CD23^{+}CD21^{int}CD93^{-}) were then sorted using a FAC SAria III (Becton Dickinson). Purity of the recovered populations was typically >98%. Follicular B cells were labeled with CFSE as previously described (Deenick et al., 1999; Avery et al., 2010) and then cultured in 24- or 48-well plates in RPMI1640 (Life Technologies) supplemented with 10% heat inactivated FCS (Life Technologies), 5 × 10^{-5} M 2-ME, 0.1 mM nonessential amino acids, 1 mM sodium pyruvate, 10 mM Hepes, 100 U/ml penicillin, 100 µg/ml Streptomycin, 100 µg/ml Noromycin (all from Sigma) at a density of 0.5 x 10^{6} cells/ml. B cells were stimulated with 10 µg/ml anti-CD40 clone FGK4.5 (Enzo Live Sciences) alone or in combination with 10 ng/ml IL-4 (R & D Systems), or 10 µg/ml LPS (Sigma) alone or together with 0.5 ng/ml TGFβ (Peprotec) and varying doses of leniolisib or equivalent doses of DMSO. After 4 d, cells were harvested and washed and stained with Zombie Aqua Viability dye (BioLegend). B cells were surface stained with B220. Cells were then fixed with 2% formalin, permeablized with saponin, and stained with mAbs to IgG1, IgG2b, and IgG3 and analyzed by flow cytometry. Some cultures were harvested and RNA prepared using an RNeasy Mini Kit (QIAGEN). PCR primers (Integrated DNA Technologies) were designed using the Roche UPL primer design program. Primer sequences and Roche UPL probes are as follows: *Aicda* UPL probe 71, forward 5′-TCCTGC TCACTGGACTTCG-3′, reverse 5′-GCGTAGGAACAACAATTCCAC-3′; *cAlpha* UPL probe 1329, 5′-TAGGGATAACAGCGCAATCC-3′, reverse 5′-GACTTTAATCGTTGAACAAACGAAC-3′. *B-actin* was quantified as a Roche Mouse Reference Gene UPL.

SW$_{HEL}$ adoptive transfers

Donor SW$_{HEL}$ *Pik3cd*^{E1020K} GOF or WT spleen cells containing 3 x 10^{4} HEL-binding B cells were injected i.v. into CD45.1 congenic C57BL/6 recipient mice along with 2 × 10^{8} SRBCs conjugated to HEL^{2X} (Brink et al., 2015). Recipient spleens and sera were harvested at the time points described. Recombinant HEL proteins (HEL^{2X} and HEL^{3X}) were produced as previously described (Brink et al., 2015). HEL^{WT} was purchased from Sigma-Aldrich. Anti-HEL antibody levels of the various Ig subclasses in the sera of recipient mice were analyzed by ELISA. 96-well ELISA plates were coated with WT HEL and bound serum Ig was detected using Ig heavy chain isotype specific Ab (BD Biosciences; biotinylated anti-IgG1 [A85-1], biotinylated anti-IgG2a/c [R19-15], biotinylated anti-IgG2b [R12-3], biotinylated anti-IgG3 [R40-82], biotinylated anti-IgM [R6-60.2]). Ig levels for each class were quantified against recombinant HyHEL10 standards (Brink et al., 2015).

Single-cell sorting and SHM analysis

Recipient spleens were prepared and stained for flow cytomtery. Donor derived IgG1 switched GC B cells were identified using anti CD45.2 PeCy7, anti-CD45.2 PerCp Cy5.5, anti-B220 PE, anti-CD38 FITC, anti IgG1-biotin, and SA-PB. Single cells were sorted using FACSAria (BD Biosciences). The variable region exon of the SW$_{HEL}$ Ig (HyHEL10) heavy chain regions was amplified by PCR and sequenced. The final product was sequenced by GEN EWIZ and analyzed.

Flow cytometry of mouse cells

The following were purchased from BD Biosciences: anti-CD45R/B220 FITC, PE, BV786 and PerCp Cy5.5, anti-CD24 PE (M1/69), anti-CD19 BV510 (1D3), biotinylated anti-CD43 (S7), biotinylated anti-IgG1(A85-1), biotinylated anti-IgG2a/c (R19-15), biotinylated anti-IgG2b (R12-3), biotinylated anti-IgG3 (R40-82), biotinylated anti-IgM (AF6-78), anti-CD16/CD32 Fc block (2.4G2), Streptavidin-BV605, Streptavidin-BV711, and Streptavidin-BUV395. The following were purchased from eBiosciences: anti-CD5 APC (53–7.3), anti-CD38 FITC (90), anti-CD45.2 PerCP-Cy5.5 (104), anti-CD45.1 PeCy7 (A20), anti-CD23 PeCy7 (B3B4), biotinylated anti-CD93 (AA4.1). The following was purchased from Invitrogen: Streptavidin-PB. The following was purchased from Life Technologies: Streptavidin-A647. The following were purchased from Biolegend: anti-IgD A647 (11-26c.2a), anti-CD93 PerCP-Cy5.5 (AA4.1), anti-IgM FITC (AF6-78), and anti-CD21/35 PB (7E9). The following were purchased from Cell Signaling Technology: anti-phospho-Akt A488 (Ser473) and PE (Thr308), anti-phospho-S6 A488 (Ser235/236).

BM and spleens of WT or *Pik3cd*^{E1020K} GOF mice, and spleens of recipient mice in adoptive transfer studies were harvested at the indicated time points, prepared and stained for flow cytometry as previously described (Chan et al., 2009). For intracellular staining of phospho-Akt or phospho-S6 cells were stained directly ex vivo for B220 then fixed in 2% formaldehyde, permeabilized in 90% methanol, and labeled with anti-phosphospecific antibodies (Avery et al., 2010). Data were acquired on either (LSR II SORP or FORTESSA; Becton Dickinson) and analyzed using FlowJo software (Tree Star). All data are representative of two or more experiments as indicated.

Statistical analysis

Significant differences were determined using Prism (GraphPad Software).

Online supplemental information

Fig. S1 shows increased phosphorylation of S6 in total B cells, increased expression of *DTX* and *LEF1* in transitional and naive B cells from patients with *PIK3CD* GOF mutations (red histograms/graphs) compared healthy donors (black histograms/graphs), and intact proliferation in vitro of control (black histograms) and *PIK3CD* GOF (red histograms) naive B cells in response to various stimuli. Fig. S2 shows differentially expressed genes in activated transitional B cells from healthy donors and patients with *PIK3CD* GOF mutations, differential expression of the indicated genes in human naive, memory, GC, and PC isolated from tonsils obtained from healthy donor, as determined by RNA Seq; differential expression of Siglec-6, CRACC, and CD27 on the surface of human tonsillar naive, memory, GC, and PC, as determined by immunofluorescent staining and flow cytometric analysis; differential expression of Siglec-6, CRACC, and CD27 on the surface of activated (i.e., CD20^{+}CD38^{-}) B cells and plasmablasts (i.e., CD20^{dim}CD38^{hi}), present in cultures of naive B cells from healthy donors cultured with CD40L/IL-21. Fig. S3 depicts increased expression of pAKT and pS6 in *Pik3cd*^{E1020K} GOF murine B cells and correction of elevated levels by the p110d inhibitor leniolisib, and proportions of total, B1, transitional, and mature B cells in the blood of WT and *Pik3cd*^{E1020K} GOF mice.

Acknowledgments

This work was supported by program grants (1016953 and 1113904 to S.G. Tangye and R. Brink; 1054925 to L.M. Corcoran), project grants (1088215 to E.K. Deenick and C.S. MaK; 1127157 to S.G. Tangye, E.K. Deenick, C.S. Ma, and T.G. Phan), Principal Research Fellowships (1042925 to S.G. Tangye; 1105877 to R. Brink), a Fulbright Senior Scholarship (S.G. Tangye), a Postgraduate Research Scholarship (1038881 to A. Kane) from the National Health and Medical Research Council of Australia, the Office of Health and Medical Research of the New South Wales Government, the Jeffrey Modell Foundation, the John Cook Brown Foundation and was made possible through Victorian State Government Operational Infrastructure Support and Australian Government National Health and Medical Research Council Independent Research Institutes Infrastructure Support Scheme Grant (361646). C.S. Ma is supported by an Early-Mid Career Research Fellowship from the New South Wales Government. W. Shi is supported by a WEHI Centenary Fellowship sponsored by Commonwealth Serum Laboratories. T. Nguyen is supported by a Research Training Program Scholarship awarded by the Australian Government.

C. Burkhart is a current employee of Novartis. None of the other authors have competing financial interests.

Author contributions D.T. Avery, A. Kane, T. Nguyen, A. Lau, H. Lenthall, K. Payne, H. Brigden, E. French, J. Bier, and D. Butt performed experiments and analyzed data; A. Nguyen and T.G. Phan analyzed microarray data; W. Shi and L.M. Corcoran provided and analyzed RNA-seq data; J.R. Hermes, D. Zahra, and R. Brink generated the *Pik3cd*^{E1020K} mutant mice; W.A. Sewell provided normal bone marrow samples; M. Elliott provided tonsil tissues; K. Boztug, I. Meyts, S. Choo, P. Hsu, M. Wong, L.J. Berglund, P. Gray, M. O'Sullivan, T. Cole, S.M. Holland, and G. Uzel provided clinical details and patient samples; C. Burkhart provided p110δ inhibitors; C.S. Ma provided intellectual input into experimental design and interpretation; E.K. Deenick and S.G. Tangye designed and supervised the project, analyzed, and interpreted data and wrote the paper. All authors edited the manuscript.

Submitted: 3 January 2018
Revised: 15 May 2018
Accepted: 20 June 2018

References

Aagaard-Tillery, K.M., and D.F. Jelinek. 1996. Phosphatidylinositol 3-kinase activation in normal human B lymphocytes. *J. Immunol.* 156:4543–4554.

Agematsu, K., H. Nagumo, F.C. Yang, T. Nakazawa, K. Fukushima, S. Ito, K. Sugita, T. Mori, T. Kobata, C. Morimoto, and A. Komiyama. 1997. B cell subpopulations separated by CD27 and crucial collaboration of CD27+ B cells and helper T cells in immunoglobulin production. *Eur. J. Immunol.* 27:2073–2079. https://doi.org/10.1002/eji.1830270835

Andjelic, S., C. Hsia, H. Suzuki, T. Kadowaki, S. Koyasu, and H.C. Liou. 2000. Phosphatidylinositol 3-kinase and NF-kappa B/Rel are at the divergence of CD40-mediated proliferation and survival pathways. *J. Immunol.* 165:3860–3867. https://doi.org/10.4049/jimmunol.165.7.3860

Angulo, I., O. Vadas, F. Garçon, E. Banham-Hall, V. Plagnol, T.R. Leahy, H. Baxendale, T. Coulter, J. Curtis, C. Wu, et al. 2013. Phosphoinositide 3-ki-

nase δ gene mutation predisposes to respiratory infection and airway damage. *Science.* 342:866–871. https://doi.org/10.1126/science.1243292

Anolik, J.H., J.W. Friedberg, B. Zheng, J. Barnard, T. Owen, E. Cushing, J. Kelly, E.C. Milner, R.I. Fisher, and I. Sanz. 2007. B cell reconstitution after rituximab treatment of lymphoma recapitulates B cell ontogeny. *Clin. Immunol.* 122:139–145. https://doi.org/10.1016/j.clim.2006.08.009

Anzelon, A.N., H. Wu, and R.C. Rickert. 2003. Pten inactivation alters peripheral B lymphocyte fate and reconstitutes CD19 function. *Nat. Immunol.* 4:287–294. https://doi.org/10.1038/ni892

Attridge, K., R. Kenefeck, L. Wardzinski, O.S. Qureshi, C.J. Wang, C. Manzotti, K. Okkenhaug, and L.S. Walker. 2014. IL-21 promotes CD4 T cell responses by phosphatidylinositol 3-kinase-dependent upregulation of CD86 on B cells. *J. Immunol.* 192:2195–2201. https://doi.org/10.4049/jimmunol.1302082

Avery, D.T., J.I. Ellyard, F. Mackay, L.M. Corcoran, P.D. Hodgkin, and S.G. Tangye. 2005. Increased expression of CD27 on activated human memory B cells correlates with their commitment to the plasma cell lineage. *J. Immunol.* 174:4034–4042. https://doi.org/10.4049/jimmunol.174.7.4034

Avery, D.T., E.K. Deenick, C.S. Ma, S. Suryani, N. Simpson, G.Y. Chew, T.D. Chan, U. Palendira, J. Bustamante, S. Boisson-Dupuis, et al. 2010. B cell-intrinsic signaling through IL-21 receptor and STAT3 is required for establishing long-lived antibody responses in humans. *J. Exp. Med.* 207:155–171. https://doi.org/10.1084/jem.20091706

Blair, P.A., L.Y. Noreña, F. Flores-Borja, D.J. Rawlings, D.A. Isenberg, M.R. Ehrenstein, and C. Mauri. 2010. CD19(+)CD24(hi)CD38(hi) B cells exhibit regulatory capacity in healthy individuals but are functionally impaired in systemic Lupus Erythematosus patients. *Immunity.* 32:129–140. https://doi.org/10.1016/j.immuni.2009.11.009

Brink, R., T.G. Phan, D. Paus, and T.D. Chan. 2008. Visualizing the effects of antigen affinity on T-dependent B-cell differentiation. *Immunol. Cell Biol.* 86:31–39. https://doi.org/10.1038/sj.icb.7100143

Brink, R., D. Paus, K. Bourne, J.R. Hermes, S. Gardam, T.G. Phan, and T.D. Chan. 2015. The SW(HEL) system for high-resolution analysis of in vivo antigen-specific T-dependent B cell responses. *Methods Mol. Biol.* 1291:103–123. https://doi.org/10.1007/978-1-4939-2498-1_9

Brunet, J.P., P. Tamayo, T.R. Golub, and J.P. Mesirov. 2004. Metagenes and molecular pattern discovery using matrix factorization. *Proc. Natl. Acad. Sci. USA.* 101:4164–4169. https://doi.org/10.1073/pnas.0308531101

Burdin, N., L. Galibert, P. Garrone, I. Durand, J. Banchereau, and F. Rousset. 1996. Inability to produce IL-6 is a functional feature of human germinal center B lymphocytes. *J. Immunol.* 156:4107–4113.

Carter, R.H., and R.A. Barrington. 2004. Signaling by the CD19/CD21 complex on B cells. *Curr. Dir. Autoimmun.* 7:4–32. https://doi.org/10.1159/000075685

Chan, T.D., D. Gatto, K. Wood, T. Camidge, A. Basten, and R. Brink. 2009. Antigen affinity controls rapid T-dependent antibody production by driving the expansion rather than the differentiation or extrafollicular migration of early plasmablasts. *J. Immunol.* 183:3139–3149. https://doi.org/10.4049/jimmunol.0901690

Clayton, E., G. Bardi, S.E. Bell, D. Chantry, C.P. Downes, A. Gray, L.A. Humphries, D. Rawlings, H. Reynolds, E. Vigorito, and M. Turner. 2002. A crucial role for the p110delta subunit of phosphatidylinositol 3-kinase in B cell development and activation. *J. Exp. Med.* 196:753–763. https://doi.org/10.1084/jem.20020805

Compagno, M., Q. Wang, C. Pighi, T.C. Cheong, F.L. Meng, T. Poggio, L.S. Yeap, E. Karaca, R.B. Blasco, F. Langellotto, et al. 2017. Phosphatidylinositol 3-kinase δ blockade increases genomic instability in B cells. *Nature.* 542:489–493. https://doi.org/10.1038/nature21406

Conley, M.E., A.K. Dobbs, A.M. Quintana, A. Bosompem, Y.D. Wang, E. Coustan-Smith, A.M. Smith, E.E. Perez, and P.J. Murray. 2012. Agammaglobulinemia and absent B lineage cells in a patient lacking the p85α subunit of PI3K. *J. Exp. Med.* 209:463–470. https://doi.org/10.1084/jem.20112533

Coulter, T.I., A. Chandra, C.M. Bacon, J. Babar, J. Curtis, N. Screaton, J.R. Goodlad, G. Farmer, C.L. Steele, T.R. Leahy, et al. 2017. Clinical spectrum and features of activated phosphoinositide 3-kinase δ syndrome: A large patient cohort study. *J. Allergy Clin. Immunol.* 139:597–606.e4. https://doi.org/10.1016/j.jaci.2016.06.021

Crank, M.C., J.K. Grossman, S. Moir, S. Pittaluga, C.M. Buckner, L. Kardava, A. Agharahimi, H. Meuwissen, J. Stoddard, J. Niemela, et al. 2014. Mutations in PIK3CD can cause hyper IgM syndrome (HIGM) associated with increased cancer susceptibility. *J. Clin. Immunol.* 34:272–276. https://doi.org/10.1007/s10875-014-0012-9

Cuss, A.K., D.T. Avery, J.L. Cannons, L.J. Yu, K.E. Nichols, P.J. Shaw, and S.G. Tangye. 2006. Expansion of functionally immature transitional B cells is associated with human-immunodeficient states characterized by impaired humoral immunity. *J. Immunol.* 176:1506–1516. https://doi.org/10.4049/jimmunol.176.3.1506

Daniel, J.A., and A. Nussenzweig. 2013. The AID-induced DNA damage response in chromatin. *Mol. Cell.* 50:309–321. https://doi.org/10.1016/j.molcel.2013.04.017

Deau, M.C., L. Heurtier, P. Frange, F. Suarez, C. Bole-Feysot, P. Nitschke, M. Cavazzana, C. Picard, A. Durandy, A. Fischer, and S. Kracker. 2014. A human immunodeficiency caused by mutations in the PIK3R1 gene. *J. Clin. Invest.* 124:3923–3928. https://doi.org/10.1172/JCI75746

Deenick, E.K., J. Hasbold, and P.D. Hodgkin. 1999. Switching to IgG3, IgG2b, and IgA is division linked and independent, revealing a stochastic framework for describing differentiation. *J. Immunol.* 163:4707–4714.

Deenick, E.K., A. Morey, M. Danta, L. Emmett, K. Fay, G. Gracie, C.S. Ma, R. Macintosh, S.A.B.C. Smith, S.C. Sasson, et al. CIRCA. 2018. Reversible Suppression of Lymphoproliferation and Thrombocytopenia with Rapamycin in a Patient with Common Variable Immunodeficiency. *J. Clin. Immunol.* 38:159–162. https://doi.org/10.1007/s10875-018-0477-z

Dengler, H.S., G.V. Baracho, S.A. Omori, S. Bruckner, K.C. Arden, D.H. Castrillon, R.A. DePinho, and R.C. Rickert. 2008. Distinct functions for the transcription factor Foxo1 at various stages of B cell differentiation. *Nat. Immunol.* 9:1388–1398. https://doi.org/10.1038/ni.1667

Dominguez-Sola, D., J. Kung, A.B. Holmes, V.A. Wells, T. Mo, K. Basso, and R. Dalla-Favera. 2015. The FOXO1 Transcription Factor Instructs the Germinal Center Dark Zone Program. *Immunity.* 43:1064–1074. https://doi.org/10.1016/j.immuni.2015.10.015

Driessen, G.J., H. IJspeert, M. Wentink, H.G. Yntema, P.M. van Hagen, A. van Strien, G. Bucciol, O. Cogulu, M. Trip, W. Nillesen, et al. 2016. Increased PI3K/Akt activity and deregulated humoral immune response in human PTEN deficiency. *J. Allergy Clin. Immunol.* 138:1744–1747.e5. https://doi.org/10.1016/j.jaci.2016.07.010

Dulau Florea, A.E., R.C. Braylan, K.T. Schafernak, K.W. Williams, J. Daub, R.K. Goyal, J.M. Puck, V.K. Rao, S. Pittaluga, S.M. Holland, et al. 2017. Abnormal B-cell maturation in the bone marrow of patients with germline mutations in PIK3CD. *J. Allergy Clin. Immunol.* 139:1032–1035.e6. https://doi.org/10.1016/j.jaci.2016.08.028

Durandy, A., N. Taubenheim, S. Peron, and A. Fischer. 2007. Pathophysiology of B-cell intrinsic immunoglobulin class switch recombination deficiencies. *Adv. Immunol.* 94:275–306. https://doi.org/10.1016/S0065-2776(06)94009-7

Eccleston, J., C. Yan, K. Yuan, F.W. Alt, and E. Selsing. 2011. Mismatch repair proteins MSH2, MLH1, and EXO1 are important for class-switch recombination events occurring in B cells that lack nonhomologous end joining. *J. Immunol.* 186:2336–2343. https://doi.org/10.4049/jimmunol.1003104

Edwards, E.S.J., J. Bier, T.S. Cole, M. Wong, P. Hsu, L.J. Berglund, K. Boztug, A. Lau, E. Gostick, D.A. Price, et al. 2018. Activating PIK3CD mutations impair human cytotoxic lymphocyte differentiation and function and EBV immunity. *J. Allergy Clin. Immunol.*:S0091-6749(18)30702-4. In press.

Elgizouli, M., D.M. Lowe, C. Speckmann, D. Schubert, J. Hülsdünker, Z. Eskandarian, A. Dudek, A. Schmitt-Graeff, J. Wanders, S.F. Jørgensen, et al. 2016. Activating PI3Kδ mutations in a cohort of 669 patients with primary immunodeficiency. *Clin. Exp. Immunol.* 183:221–229. https://doi.org/10.1111/cei.12706

Elkaim, E., B. Neven, J. Bruneau, K. Mitsui-Sekinaka, A. Stanislas, L. Heurtier, C.L. Lucas, H. Matthews, M.C. Deau, S. Sharapova, et al. 2016. Clinical and immunologic phenotype associated with activated phosphoinositide 3-kinase δ syndrome 2: A cohort study. *J. Allergy Clin. Immunol.* 138:210–218.e9. https://doi.org/10.1016/j.jaci.2016.03.022

Ellyard, J.I., D.T. Avery, T.G. Phan, N.J. Hare, P.D. Hodgkin, and S.G. Tangye. 2004. Antigen-selected, immunoglobulin-secreting cells persist in human spleen and bone marrow. *Blood.* 103:3805–3812. https://doi.org/10.1182/blood-2003-09-3109

Fruman, D.A., S.B. Snapper, C.M. Yballe, L. Davidson, J.Y. Yu, F.W. Alt, and L.C. Cantley. 1999. Impaired B cell development and proliferation in absence of phosphoinositide 3-kinase p85alpha. *Science.* 283:393–397. https://doi.org/10.1126/science.283.5400.393

Fruman, D.A., H. Chiu, B.D. Hopkins, S. Bagrodia, L.C. Cantley, and R.T. Abraham. 2017. The PI3K Pathway in Human Disease. *Cell.* 170:605–635. https://doi.org/10.1016/j.cell.2017.07.029

Good, K.L., V.L. Bryant, and S.G. Tangye. 2006. Kinetics of human B cell behavior and amplification of proliferative responses following stimulation with IL-21. *J. Immunol.* 177:5236–5247. https://doi.org/10.4049/jimmunol.177.8.5236

Good, K.L., D.T. Avery, and S.G. Tangye. 2009. Resting human memory B cells are intrinsically programmed for enhanced survival and responsiveness to diverse stimuli compared to naive B cells. *J. Immunol.* 182:890–901. https://doi.org/10.4049/jimmunol.182.2.890

Goodnow, C.C. 2007. Multistep pathogenesis of autoimmune disease. *Cell.* 130:25–35. https://doi.org/10.1016/j.cell.2007.06.033

Goodnow, C.C., C.G. Vinuesa, K.L. Randall, F. Mackay, and R. Brink. 2010. Control systems and decision making for antibody production. *Nat. Immunol.* 11:681–688. https://doi.org/10.1038/ni.1900

Hartman, H.N., J. Niemela, M.K. Hintermeyer, M. Garofalo, J. Stoddard, J.W. Verbsky, S.D. Rosenzweig, and J.M. Routes. 2015. Gain of Function Mutations of PIK3CD as a Cause of Primary Sclerosing Cholangitis. *J. Clin. Immunol.* 35:11–14. https://doi.org/10.1007/s10875-014-0109-1

Hasbold, J., A.B. Lyons, M.R. Kehry, and P.D. Hodgkin. 1998. Cell division number regulates IgG1 and IgE switching of B cells following stimulation by CD40 ligand and IL-4. *Eur. J. Immunol.* 28:1040–1051. https://doi.org/10.1002/(SICI)1521-4141(199803)28:03%3C1040::AID-IMMU1040%3E3.0.CO;2-9

Hasbold, J., L.M. Corcoran, D.M. Tarlinton, S.G. Tangye, and P.D. Hodgkin. 2004. Evidence from the generation of immunoglobulin G-secreting cells that stochastic mechanisms regulate lymphocyte differentiation. *Nat. Immunol.* 5:55–63. https://doi.org/10.1038/ni1016

Hewett, Y.G., D. Uprety, and B.K. Shah. 2016. Idelalisib- a PI3Kδ targeting agent for B-cell malignancies. *J. Oncol. Pharm. Pract.* 22:284–288. https://doi.org/10.1177/1078155215572933

Hodgkin, P.D., J.H. Lee, and A.B. Lyons. 1996. B cell differentiation and isotype switching is related to division cycle number. *J. Exp. Med.* 184:277–281. https://doi.org/10.1084/jem.184.1.277

Hoegenauer, K., N. Soldermann, F. Zécri, R.S. Strang, N. Graveleau, R.M. Wolf, N.G. Cooke, A.B. Smith, G.J. Hollingworth, J. Blanz, et al. 2017. Discovery of CDZ173 (Leniolisib), Representing a Structurally Novel Class of PI3K Delta-Selective Inhibitors. *ACS Med. Chem. Lett.* 8:975–980. https://doi.org/10.1021/acsmedchemlett.7b00293

Jou, S.T., N. Carpino, Y. Takahashi, R. Piekorz, J.R. Chao, N. Carpino, D. Wang, and J.N. Ihle. 2002. Essential, nonredundant role for the phosphoinositide 3-kinase p110delta in signaling by the B-cell receptor complex. *Mol. Cell. Biol.* 22:8580–8591. https://doi.org/10.1128/MCB.22.24.8580-8591.2002

Jou, S.T., Y.H. Chien, Y.H. Yang, T.C. Wang, S.D. Shyur, C.C. Chou, M.L. Chang, D.T. Lin, K.H. Lin, and B.L. Chiang. 2006. Identification of variations in the human phosphoinositide 3-kinase p110delta gene in children with primary B-cell immunodeficiency of unknown aetiology. *Int. J. Immunogenet.* 33:361–369. https://doi.org/10.1111/j.1744-313X.2006.00627.x

Jourdan, M., A. Caraux, G. Caron, N. Robert, G. Fiol, T. Rème, K. Bolloré, J.P. Vendrell, S. Le Gallou, F. Mourcin, et al. 2011. Characterization of a transitional preplasmablast population in the process of human B cell to plasma cell differentiation. *J. Immunol.* 187:3931–3941. https://doi.org/10.4049/jimmunol.1101230

Jung, J., J. Choe, L. Li, and Y.S. Choi. 2000. Regulation of CD27 expression in the course of germinal center B cell differentiation: the pivotal role of IL-10. *Eur. J. Immunol.* 30:2437–2443. https://doi.org/10.1002/1521-4141(2000)30:8%3C2437::AID-IMMU2437%3E3.0.CO;2-M

Kallies, A., J. Hasbold, K. Fairfax, C. Pridans, D. Emslie, B.S. McKenzie, A.M. Lew, L.M. Corcoran, P.D. Hodgkin, D.M. Tarlinton, and S.L. Nutt. 2007. Initiation of plasma-cell differentiation is independent of the transcription factor Blimp-1. *Immunity.* 26:555–566. https://doi.org/10.1016/j.immuni.2007.04.007

Kardava, L., S. Moir, W. Wang, J. Ho, C.M. Buckner, J.G. Posada, M.A. O'Shea, G. Roby, J. Chen, H.W. Sohn, et al. 2011. Attenuation of HIV-associated human B cell exhaustion by siRNA downregulation of inhibitory receptors. *J. Clin. Invest.* 121:2614–2624. https://doi.org/10.1172/JCI45685

Kim, H., and H. Park. 2007. Sparse non-negative matrix factorizations via alternating non-negativity-constrained least squares for microarray data analysis. *Bioinformatics.* 23:1495–1502. https://doi.org/10.1093/bioinformatics/btm134

Kracker, S., J. Curtis, M.A. Ibrahim, A. Sediva, J. Salisbury, V. Campr, M. Debré, J.D. Edgar, K. Imai, C. Picard, et al. 2014. Occurrence of B-cell lymphomas in patients with activated phosphoinositide 3-kinase δ syndrome. *J. Allergy Clin. Immunol.* 134:233–236. https://doi.org/10.1016/j.jaci.2014.02.020

Law, C.W., Y. Chen, W. Shi, and G.K. Smyth. 2014. voom: Precision weights unlock linear model analysis tools for RNA-seq read counts. *Genome Biol.* 15:R29. https://doi.org/10.1186/gb-2014-15-2-r29

LeBien, T.W., and T.F. Tedder. 2008. B lymphocytes: how they develop and function. *Blood.* 112:1570–1580. https://doi.org/10.1182/blood-2008-02-078071

Liao, Y., G.K. Smyth, and W. Shi. 2013. The Subread aligner: fast, accurate and scalable read mapping by seed-and-vote. *Nucleic Acids Res.* 41:e108. https://doi.org/10.1093/nar/gkt214

Liao, Y., G.K. Smyth, and W. Shi. 2014. featureCounts: an efficient general purpose program for assigning sequence reads to genomic features. *Bioinformatics.* 30:923–930. https://doi.org/10.1093/bioinformatics/btt656

Lucas, C.L., H.S. Kuehn, F. Zhao, J.E. Niemela, E.K. Deenick, U. Palendira, D.T. Avery, L. Moens, J.L. Cannons, M. Biancalana, et al. 2014a. Dominant-activating germline mutations in the gene encoding the PI(3)K catalytic subunit p110δ result in T cell senescence and human immunodeficiency. *Nat. Immunol.* 15:88–97. https://doi.org/10.1038/ni.2771

Lucas, C.L., Y. Zhang, A. Venida, Y. Wang, J. Hughes, J. McElwee, M. Butrick, H. Matthews, S. Price, M. Biancalana, et al. 2014b. Heterozygous splice mutation in PIK3R1 causes human immunodeficiency with lymphoproliferation due to dominant activation of PI3K. *J. Exp. Med.* 211:2537–2547. https://doi.org/10.1084/jem.20141759

Moens, L., and S.G. Tangye. 2014. Cytokine-Mediated Regulation of Plasma Cell Generation: IL-21 Takes Center Stage. *Front. Immunol.* 5:65. https://doi.org/10.3389/fimmu.2014.00065

Morbach, H., E.M. Eichhorn, J.G. Liese, and H.J. Girschick. 2010. Reference values for B cell subpopulations from infancy to adulthood. *Clin. Exp. Immunol.* 162:271–279. https://doi.org/10.1111/j.1365-2249.2010.04206.x

Okkenhaug, K. 2013. Signaling by the phosphoinositide 3-kinase family in immune cells. *Annu. Rev. Immunol.* 31:675–704. https://doi.org/10.1146/annurev-immunol-032712-095946

Okkenhaug, K., and B. Vanhaesebroeck. 2003. PI3K in lymphocyte development, differentiation and activation. *Nat. Rev. Immunol.* 3:317–330. https://doi.org/10.1038/nri1056

Okkenhaug, K., A. Bilancio, G. Farjot, H. Priddle, S. Sancho, E. Peskett, W. Pearce, S.E. Meek, A. Salpekar, M.D. Waterfield, et al. 2002. Impaired B and T cell antigen receptor signaling in p110delta PI 3-kinase mutant mice. *Science.* 297:1031–1034.

Omori, S.A., M.H. Cato, A. Anzelon-Mills, K.D. Puri, M. Shapiro-Shelef, K. Calame, and R.C. Rickert. 2006. Regulation of class-switch recombination and plasma cell differentiation by phosphatidylinositol 3-kinase signaling. *Immunity.* 25:545–557. https://doi.org/10.1016/j.immuni.2006.08.015

Ostiguy, V., E.L. Allard, M. Marquis, J. Leignadier, and N. Labrecque. 2007. IL-21 promotes T lymphocyte survival by activating the phosphatidylinositol-3 kinase signaling cascade. *J. Leukoc. Biol.* 82:645–656. https://doi.org/10.1189/jlb.0806494

Palanichamy, A., J. Barnard, B. Zheng, T. Owen, T. Quach, C. Wei, R.J. Looney, I. Sanz, and J.H. Anolik. 2009. Novel human transitional B cell populations revealed by B cell depletion therapy. *J. Immunol.* 182:5982–5993. https://doi.org/10.4049/jimmunol.0801859

Patel, N., E.C. Brinkman-Van der Linden, S.W. Altmann, K. Gish, S. Balasubramanian, J.C. Timans, D. Peterson, M.P. Bell, J.F. Bazan, A. Varki, and R.A. Kastelein. 1999. OB-BP1/Siglec-6. a leptin- and sialic acid-binding protein of the immunoglobulin superfamily. *J. Biol. Chem.* 274:22729–22738. https://doi.org/10.1074/jbc.274.32.22729

Rao, V.K., S. Webster, V.A.S.H. Dalm, A. Šedivá, P.M. van Hagen, S. Holland, S.D. Rosenzweig, A.D. Christ, B. Sloth, M. Cabanski, et al. 2017. Effective "activated PI3Kδ syndrome"-targeted therapy with the PI3Kδ inhibitor leniolisib. *Blood.* 130:2307–2316. https://doi.org/10.1182/blood-2017-08-801191

Ren, C.L., T. Morio, S.M. Fu, and R.S. Geha. 1994. Signal transduction via CD40 involves activation of lyn kinase and phosphatidylinositol-3-kinase, and phosphorylation of phospholipase C gamma 2. *J. Exp. Med.* 179:673–680. https://doi.org/10.1084/jem.179.2.673

Ritchie, M.E., B. Phipson, D. Wu, Y. Hu, C.W. Law, W. Shi, and G.K. Smyth. 2015. limma powers differential expression analyses for RNA-sequencing and microarray studies. *Nucleic Acids Res.* 43:e47. https://doi.org/10.1093/nar/gkv007

Rolf, J., S.E. Bell, D. Kovesdi, M.L. Janas, D.R. Soond, L.M. Webb, S. Santinelli, T. Saunders, B. Hebeis, N. Killeen, et al. 2010. Phosphoinositide 3-kinase activity in T cells regulates the magnitude of the germinal center reaction. *J. Immunol.* 185:4042–4052. https://doi.org/10.4049/jimmunol.1001730

Ruiz-García, R., A. Vargas-Hernández, I.K. Chinn, L.S. Angelo, T.N. Cao, Z. Coban-Akdemir, S.N. Jhangiani, Q. Meng, L.R. Forbes, D.M. Muzny, et al. 2018. Mutations in PI3K110δ cause impaired natural killer cell function partially rescued by rapamycin treatment. *J. Allergy Clin. Immunol.*:S0091-6749(18)30026-5.

Sander, S., V.T. Chu, T. Yasuda, A. Franklin, R. Graf, D.P. Calado, S. Li, K. Imami, M. Selbach, M. Di Virgilio, et al. 2015. PI3 Kinase and FOXO1 Transcription Factor Activity Differentially Control B Cells in the Germinal Center Light and Dark Zones. *Immunity.* 43:1075–1086. https://doi.org/10.1016/j.immuni.2015.10.021

Sims, G.P., R. Ettinger, Y. Shirota, C.H. Yarboro, G.G. Illei, and P.E. Lipsky. 2005. Identification and characterization of circulating human transitional B cells. *Blood.* 105:4390–4398. https://doi.org/10.1182/blood-2004-11-4284

Smyth, G.K. 2004. Linear models and empirical bayes methods for assessing differential expression in microarray experiments. *Stat. Appl. Genet. Mol. Biol.* 3:e3. https://doi.org/10.2202/1544-6115.1027

Srinivasan, L., Y. Sasaki, D.P. Calado, B. Zhang, J.H. Paik, R.A. DePinho, J.L. Kutok, J.F. Kearney, K.L. Otipoby, and K. Rajewsky. 2009. PI3 kinase signals BCR-dependent mature B cell survival. *Cell.* 139:573–586. https://doi.org/10.1016/j.cell.2009.08.041

Suryani, S., D.A. Fulcher, B. Santner-Nanan, R. Nanan, M. Wong, P.J. Shaw, J. Gibson, A. Williams, and S.G. Tangye. 2010. Differential expression of CD21 identifies developmentally and functionally distinct subsets of human transitional B cells. *Blood.* 115:519–529. https://doi.org/10.1182/blood-2009-07-234799

Suzuki, A., T. Kaisho, M. Ohishi, M. Tsukio-Yamaguchi, T. Tsubata, P.A. Koni, T. Sasaki, T.W. Mak, and T. Nakano. 2003. Critical roles of Pten in B cell homeostasis and immunoglobulin class switch recombination. *J. Exp. Med.* 197:657–667. https://doi.org/10.1084/jem.20021101

Suzuki, H., Y. Terauchi, M. Fujiwara, S. Aizawa, Y. Yazaki, T. Kadowaki, and S. Koyasu. 1999. Xid-like immunodeficiency in mice with disruption of the p85alpha subunit of phosphoinositide 3-kinase. *Science.* 283:390–392. https://doi.org/10.1126/science.283.5400.390

Tang, P., J.E.M. Upton, M.A. Barton-Forbes, M.I. Salvadori, M.P. Clynick, A.K. Price, and S.L. Goobie. 2018. Autosomal Recessive Agammaglobulinemia Due to a Homozygous Mutation in PIK3R1. *J. Clin. Immunol.* 38:88–95. https://doi.org/10.1007/s10875-017-0462-y

Tangye, S.G., C.S. Ma, R. Brink, and E.K. Deenick. 2013. The good, the bad and the ugly - TFH cells in human health and disease. *Nat. Rev. Immunol.* 13:412–426. https://doi.org/10.1038/nri3447

Tangye, S.G., R. Brink, C.C. Goodnow, and T.G. Phan. 2015. SnapShot: Interactions between B Cells and T Cells. *Cell.* 162:926–6.e1. https://doi.org/10.1016/j.cell.2015.07.055

Tsujita, Y., K. Mitsui-Sekinaka, K. Imai, T.W. Yeh, N. Mitsuiki, T. Asano, H. Ohnishi, Z. Kato, Y. Sekinaka, K. Zaha, et al. 2016. Phosphatase and tensin homolog (PTEN) mutation can cause activated phosphatidylinositol 3-kinase δ syndrome-like immunodeficiency. *J. Allergy Clin. Immunol.* 138:1672–1680.e10. https://doi.org/10.1016/j.jaci.2016.03.055

Uckun, F.M. 1990. Regulation of human B-cell ontogeny. *Blood.* 76:1908–1923.

van Zelm, M.C., M. van der Burg, D. de Ridder, B.H. Barendregt, E.F. de Haas, M.J. Reinders, A.C. Lankester, T. Révész, F.J. Staal, and J.J. van Dongen. 2005. Ig gene rearrangement steps are initiated in early human precursor B cell subsets and correlate with specific transcription factor expression. *J. Immunol.* 175:5912–5922. https://doi.org/10.4049/jimmunol.175.9.5912

Xu, Z.Z., Z.G. Xia, A.H. Wang, W.F. Wang, Z.Y. Liu, L.Y. Chen, and J.M. Li. 2013. Activation of the PI3K/AKT/mTOR pathway in diffuse large B cell lymphoma: clinical significance and inhibitory effect of rituximab. *Ann. Hematol.* 92:1351–1358. https://doi.org/10.1007/s00277-013-1770-9

Yang, H., H. Wang, and R. Jaenisch. 2014. Generating genetically modified mice using CRISPR/Cas-mediated genome engineering. *Nat. Protoc.* 9:1956–1968. https://doi.org/10.1038/nprot.2014.134

Zeng, R., R. Spolski, E. Casas, W. Zhu, D.E. Levy, and W.J. Leonard. 2007. The molecular basis of IL-21-mediated proliferation. *Blood.* 109:4135–4142. https://doi.org/10.1182/blood-2006-10-054973